Supplement of

Does Nonstationarity in Rainfall Requires Nonstationary Intensity-Duration-Frequency Curves?

Poulomi Ganguli[1], Paulin Coulibaly[1]

[1]Department of Civil Engineering, McMaster Water Resources and Hydrologic Modelling Group, McMaster University, 1280 Main Street West, Hamilton, ON L8S 4L7, Canada

Correspondence to: Poulomi Ganguli (poulomi.ganguli@alumnimail.iitkgp.ac.in; gangulip@mcmaster.ca)

Table S1. Selected station locations, population distribution and hourly and daily data availability

Stations	EC-Station ID	Lat (°)	Long (°)	Elevation (m)	Population Estimate	Census Subdivision	EC-derived Annual Maxima Rainfall	Hourly Rainfall	Daily Rainfall
Toronto P. Int'l Airport	6158731	43.68	-79.63	173.4	5,583,046	Toronto CMA[1]	1950 - 2013	1960 - 2012	1940 - 2013
Hamilton Airport	6153194	43.17	-79.93	237.7	519,949	Population Center	1971 - 2003	1971 - 2003	1960 – 2010
Oshawa WPCP	6155878	43.87	-78.83	83.8	356,177	Oshawa CMA	1970 - 2006	1970 – 1999	1970 - 2015
Windsor Airport	6139525	42.28	-82.96	189.6	319,246	Windsor CMA	1946 - 2007	1960 – 2007	1940 - 2013
Kingston P. Station	6104175	44.24	-76.48	76.5	159,561	Kingston CMA	1961 - 2007	1961 – 2003	1960 – 2007
London Int'l Airport	6144478/75	43.03	-81.15	278	474,786	London CMA	1950 - 2007*	1961 – 2001	1940 – 2015
Trenton Airport	6158875	44.12	-77.53	86.3	43,086	Population Center	1965 - 2013	1964 – 1997	1935 – 2015
Stratford WWTP	6148100	43.37	-81.0	345	30,886	CA	1966 - 2004	1966 – 2007	1960 – 2015
Fergus Shand Dam	6142400	43.73	-80.33	417.6	19,126	Population Center	1961 - 2007	1960 – 2007	1950 – 2015

[1] CMA and CA denote census metropolitan area and census agglomeration respectively. Statistics of Canada defines a CMA with a population of at least 100,000, where the urban core of that area has at least 50,000 people, whereas CA must have an urban core population of at least 10, 000. From 2011 census onwards, the term urban area is replaced with *population center*. A population center is an area with at least a population of 1,000 and a density of 400 or more people per square kilometer. All population information are collected from Statistics Canada (https://www12.statcan.gc.ca/) website. *Missing values are infilled using observations from nearest Environment Canada station ID 6144475 (latitude 44° and longitude -81.5°) located at 111.5 km geodesic distance.

SI 1. Multiplicative Random Cascade (MRC) Models for Temporal Disaggregation of Rainfall

Multiplicative random cascades were first developed for studies of turbulence (Mandelbrot, 1999; Yaglom, 1966) with a motivation to have mathematical models, which produce time series that have statistically scale-invariant properties. In general, random cascade model for rainfall assumes a division of known rainfall total R_L occurring over an interval of time among a number of smaller intervals of fixed size, which implies a successive fine graining process that starts from an original, large scale resolution R_L and continues till a target small scale resolution is reached. The approach is based on scaling laws, which describe the scale-invariant properties or relationships that connect the statistical properties of rainfall for different time scales (Willems, 2012). The number of subintervals is defined by the branching number *b*, is set to 2, which is a redistribution of total rainfall in period *i* at a resolution r, $R_{i,r}$, between the amount associated with the first and last half respectively.

Here we implement a micro-canonical (exact conservation of mass in each cascade branching) cascade-based temporal disaggregation model as proposed by (Olsson, 1998), in which daily rainfall is disaggregated using a uniformly distributed generator, dependent on rainfall intensity and position of the rain sequence. The technique was later successfully implemented by (Güntner et al., 2001; Jebari et al., 2012; Rana et al., 2013) for temporal disaggregation of point rainfall and the development of IDF-curves from short-duration rainfall extremes. In the disaggregation process, each time interval (box) at a given resolution (for example 1 day) is split into two half of the original length (1/2 day). The procedure is continued as a cascade until the desired time resolution is reached, i.e., to ¼ day, then to 1/8 of a day and so on. Each step is termed as a cascade step, with cascade step 0 as the longest time period with only one box (*i.e.*, a day). The distribution of the volume between two sub-intervals (or smaller boxes) is computed by multiplication with the cascade weights ($W_{i,r}$), $0 \le W_{i,r} \le 1$ that assigns $W_{i,r} \bullet R_{i,r}$ to the first half of the period and $\left(1 - W_{i,r}\right) \bullet R_{i,r}$ to the next half. In each branching two possibilities exist: (1) $W_1 = 0$, $W_1 = 1$ (2) $0 < W_1 < 1$. The occurrence of (1) and (2) may be expressed in terms of probabilities, $P_{01} = P_{(1/0)}$ or $P_{(0/1)}$ = P($W_1 = 0$ or $W_1 = 1$) and $P_{xx} = P_{(x/x)}$ = P($0 < W_1 < 1$) = 1 - P_{01}.

Depending on the range of resolution involve, P_{01} either be assumed as resolution independent or parameterized as a scaling law: $Pr_{01}(r) = c_1 r^{c_2}$ where c_1 and c_2 are constants. The distribution of $W_{i,r}$ is termed as cascade generator, assumed to follow 1-parameter beta distribution

(Olsson, n.d.). Following (Olsson, 1998), the probabilities *P*, the probability distribution of cascade generator are assumed to be related to (1) position in rainfall sequence, and (2) rainfall volume. The wet boxes, with a rainfall volume $V > 0$, can be characterized by their position in the rainfall series: (1) the starting box, box preceded by a dry box ($V = 0$) and succeeded by a wet box ($V > 0$); (2) the enclosed box, box preceded and succeeded by wet boxes; (3) the ending box, box preceded by a wet box and succeeded by a dry box, and (4) the isolated box, box preceded and succeeded by dry boxes. On the other hand, based on volume dependence, if the volume is large then it is more likely that both halves of the subintervals contribute to nonzero volume than if the volume is small. Following (Olsson, 1998), a partition into three volume classes ($v_c = 1, 2, 3$) was used, separated by percentiles 33rd and 67th of the values at the cascade step. Next, the variation of $P_{(x/x)}$ with volume is parameterised as, $P_{(x/x)} = a + b_m \bullet v_c$, where *a* is the intercept at $v_c = 0$, b_m is the mean slope of linear regression obtained from all cascade steps and v_c is volume class. For details about theory and implementation issues of MRC-based disaggregation tool, interested readers are requested to refer (Olsson, 1998).

For calibration and application of the disaggregated model from an original resolution R_l, two situations are considered: (1) when representative data at target resolution R_s is available; such as in this case, disaggregation from daily to hourly time steps, in which hourly data were available. Hence, parameters are calibrated over the actual resolution interval $R_l < r < R_s$ using 5 cascade steps. This implies, 5 successive "halving" from one day to generate 45-minute (2700 seconds) data. (2) When no representative high-resolution data are available, then parameters are estimated by coarse graining from lower resolution R_l to a higher resolution R_s by successive disaggregation steps. In this study, it is the disaggregation from daily to minute scales (or sub-hourly time steps), in which no sub-hourly data were available for any of the representative sites. In such case, parameters are calibrated from daily rainfall data using 7 cascade steps. This implies disaggregating by halving from 1-day to 11-minute 15 second (675 seconds) data. After calibration, Monte Carlo simulation is performed to gradually fine-grain the data and generate realizations at desired resolution, R_s. Since R_s in these cases are not directly achieved by exact resolution doubling from R_l, the target resolutions are obtained by geometric interpolation of the disaggregated model output at the final time step. In the next sub-sections, we demonstrate the performance of the MRC-based disaggregation tool using two different sets of observations.

S (A) Performance Evaluation of MRC-based disaggregation Tools for McMaster Weather Station Data

McMaster weather station is situated on a rooftop of McMaster University campus (43.26° N latitude and 79.92° W longitude, 114 m above sea level). We obtain daily, hourly and sub-hourly (15-min) rainfall information from the year 2010 to 2013, archived at McMaster Weather Station (MUWS; http://geomedia.mcmaster.ca/muws/weatherstation.html) website. The time slice was chosen based on data completeness and quality of available records.

We investigate two cases: (1) First, we calibrate the model using 1-year (2012 – 2013) hourly data, estimated model parameters, and then assess the performance of disaggregated model output using 2010 – 2013 observed data (2) Next, the observed 15-min time series was first aggregated to an hourly time step and then calibrated the model using aggregated hourly data. Then we compare disaggregated versus observed data at a 15-min temporal resolution for validation. Since we do not have 15-min daily rainfall information available for any of rain gauge locations, in both cases we calibrate the model using hourly data, which in turn gives us the opportunity to evaluate the performance of the disaggregation algorithm. In all cases, disaggregation was performed from daily time scales. Table S2 shows results of disaggregation experiments. We find a satisfactory performance between observed and simulated model output, especially for the simulation of the percentage of zero values. However, we find a slight underestimation for simulated standard deviations of event volume and duration, whereas variance of mean inter-arrival time is overestimated.

Table S2. Comparison between observed and disaggregated 15-min and 1-hour time series for McMaster Weather Station Data

Time scale	Metrics	Observed	Simulated
Hourly (1-hr)	Zero values (%)	92	91.5
	Individual Rainfall volume (mean ± SD) mm	1.60 ± 2.95	1.45 ± 2.89
	Event volume (mean ± SD) mm	4.52 ± 10.40	4.50 ± 8.82
	Event duration (mean ± SD) hour	2.83 ± 3.51	3.09 ± 2.69
	Mean inter-arrival time between event, hour	36.82 ± 64.70	37.33 ± 65.10
	Mean annual maxima (mean ± SD) mm	39.97 ± 21.42	32.97 ± 12.33
Minute (15-min)	Zero values (%)	94.63	95.35
	Individual Rainfall volume (mean ± SD) mm	0.032 ± 1.20	0.031 ± 1.28
	Event volume (mean ± SD) mm	1.87 ± 6.28	1.96 ± 4.64
	Event duration (mean ± SD) hour	3.15 ± 5.77	2.94 ± 3.47
	Mean inter-arrival time between event, hour	59.54 ± 177.33	64.12 ± 182.01
	Mean annual maxima (mean ± SD) mm	20.4 ± 10.22	23.4 ± 12.70

S (B) Performance Evaluation of MRC-based disaggregation Tools for the Nine Locations in Southern Ontario

Figure S3 – S7 displays disaggregation fit of the MRC-based tools for Toronto International Airport. Figures S3 and S4 show variations of probability with volume classes, which often show substantial differences between the classes. The figures show a linear relationship between precipitation, P and volume class, v_c changes with cascade steps. The mean regression line $a_p + b_m * vc$, (where a_p is the intercept and b_m is the slope) is shown as a dashed line with squares (Figure S3). Figures S4 and S5 show variations of intercepts with cascade steps. The probabilities P(x/x) and P(0/1) for daily to minute-scale disaggregation of four different type of boxes are shown in Tables S2 and S3. P(x/x) can be modelled assuming linear dependence on the cascade step, which is given as, $P(x/x) = a_p + b_m * vc$ with a_p is estimated as, $a_p = c_1 + c_2 * C_s$, where c_1 and c_2 are the slope and the intercept of the linear regression. Since P(0/1) [or P(1/0)] is relatively independent of cascade step, it can be modeled using $a_p + b_m * vc$. Finally, P(0/1) [or P(1/0)] can be estimated as, P(0/1)=1-(P(x/x)+P(1/0) [or P(1/0)=1-(P(x/x)+P(0/1)]. The empirical histograms (the observed, shown in bars) and the fitted beta distributions (shown in lines) [Figures S6 and S7] show a good agreement in the overall

fit. However, at higher cascade steps, i.e. finer time scales, the number of bins in the histogram is small, and the fits appear naturally uncertain.

Figure S8 shows time series of disaggregated versus observed annual maxima (the 15-min and 1-hour) for Toronto International Airport. The quantile mapping (QM) is employed to adjust occasional overestimation due to disaggregation. Except for a few extremes, we find a close agreement between the observed versus bias-corrected disaggregated annual maxima time series. For example, the algorithm overestimates the wettest event in Toronto (137.4 mm of rainfall) during Hurricane Hazel (1954) at hourly disaggregation time steps. However, due to lack of observation, we could not validate 15-min disaggregation model performance. Figure S9 shows 1-hour disaggregated model performance for the nine sites. Although we find evidence of occasional overestimations in disaggregated model output, the adjustment of extremes by QM could correct biases to some extent. However, the algorithm fails to correct extreme wet biases for London International Airport (during 1954), Trenton Airport (2000), Stratford WWTP (2002) and Fergus Shand Dam (2004 and 2006).

Table S3. Probabilities $P(x/x)$ as function of volume class, cascade step and type of box for daily to minute scale disaggregation

Volume Class/Cascade Step	**1**	**2**	**3**	**4**	**5**	**6**	**7**	Mean
1. Isolated Box (b_m = 0.223)								
1	0.001	0.030	0.051	0.048	0.073	0.082	0.031	0.045
2	0.244	0.254	0.266	0.299	0.249	0.289	0.267	0.27
3	0.509	0.505	0.510	0.513	0.512	0.470	0.420	0.49
2. Starting Box (b_m = 0.244)								
1	0.054	0.122	0.081	0.064	0.101	0.130	0.095	0.092
2	0.399	0.415	0.345	0.290	0.275	0.283	0.437	0.349
3	0.635	0.612	0.610	0.527	0.487	0.570	0.628	0.581
3. Enclosed Box (b_m = 0.263)								
1	0.423	0.357	0.272	0.157	0.097	0.156	0.194	0.236
2	0.862	0.817	0.703	0.510	0.335	0.345	0.463	0.576
3	0.951	0.938	0.875	0.736	0.585	0.562	0.685	0.762
4. Ending Box (b_m = 0.247)								
1	0.063	0.033	0.064	0.087	0.084	0.109	0.114	0.079
2	0.381	0.372	0.323	0.253	0.303	0.237	0.439	0.330
3	0.651	0.639	0.591	0.564	0.474	0.496	0.593	0.572

Table S4. Probabilities *P*(0/1) as function of volume class, cascade step and type of box for daily to minute scale disaggregation

Volume Class/Cascade Step	1	2	3	4	5	6	7	Mean
1. Isolated Box (b_m = -0.113)								
1	0.446	0.449	0.494	0.466	0.427	0.482	0.50	0.466
2	0.369	0.388	0.370	0.330	0.400	0.369	0.30	0.361
3	0.257	0.248	0.236	0.242	0.241	0.259	0.193	0.239
2. Starting Box (b_m = -0.175)								
1	0.747	0.713	0.771	0.711	0.681	0.565	0.526	0.673
2	0.535	0.521	0.583	0.593	0.558	0.409	0.295	0.499
3	0.320	0.333	0.347	0.408	0.394	0.274	0.195	0.324
3. Enclosed Box (b_m = -0.113)								
1	0.272	0.283	0.330	0.387	0.400	0.405	0.374	0.350
2	0.078	0.103	0.159	0.220	0.350	0.348	0.253	0.216
3	0.027	0.031	0.077	0.154	0.204	0.224	0.158	0.125
4. Ending Box (b_m = -0.068)								
1	0.215	0.211	0.167	0.202	0.210	0.330	0.298	0.233
2	0.093	0.083	0.098	0.144	0.187	0.318	0.263	0.169
3	0.040	0.054	0.068	0.072	0.120	0.174	0.159	0.098

SI 2 Non-parametric Trend Free Pre-Whitening (TPFW) for Correction of Autocorrelation

To correct the autocorrelation present in the data, we followed the non-parametric procedure of trend-free pre-whitening (TPFW) as suggested by the (Petrow and Merz, 2009):

- At first, the trend of annual maxima time series of a particular duration is estimated by the non-parametric trend slope estimator, β as suggested by (Sen, 1968), which is the median of all pair wise slopes (b_i) in the time series of length (N):

$$\beta = \begin{cases} b_{(N+1)/2} & if\ N\ is\ odd \\ \frac{1}{2}\left(b_{N/2} + b_{(N+1)/2}\right) & if\ N\ is\ even \end{cases} \tag{2.1}$$

Where, $b_i = \frac{\left(x_j - x_k\right)}{j-k}$, $i = 1, 2, ..., N\ and\ j > k$, and x_j and x_k are the data points in time periods j and k ($j > k$) respectively. Hence, if there are n values of data in the time series, it results into as many as $N = {}^{n}C_2$ number of b_i values.

- Secondly, the computed trend is removed from the original series:

$$Y_t = X_t - \beta \times t \tag{2.2}$$

Where, X_t is the original time series and t is the time.

- Next, the lag1- autocorrelation [ρ, using MATLAB function 'autocorr ()'], is computed from Y_t. If no statistically significant (significance is checked at 5 and 10% significance level) autocorrelation is found, the trend and change-point detection algorithms are directly applied to the original time series. Otherwise, the lag-1 autocorrelation is removed from the time series:

$$Y_t' = Y_t - \rho \times Y_{t-1} \tag{2.3}$$

- Finally, the removed trend in the first step is added back into the time series free from trend and autocorrelation.

$$Y_t'' = Y_t' + \beta \times t \tag{2.4}$$

The resulting time series Y'' includes the original trend but free from autocorrelation.

SI 3 Generalized Extreme Value (GEV) Distribution Function (DF)

The cumulative DFs of stationary (time invariant) GEV model is given by (Coles et al., 2001):

$$G(z) = \exp\left\{-\left[1+\zeta\left(\frac{z-\mu}{\sigma}\right)\right]_+^{-1/\zeta}\right\} \qquad \sigma > 0, -\infty < \mu, \zeta < \infty \tag{3.1}$$

Where, $y_+ = \max\{y, 0\}$, μ is a location parameter, σ is a scale parameter and ζ is a shape parameter determining the heaviness of the tail. The shape parameter ζ, determines the higher moments of the density function and also the skew in the probability mass. The '+' sign indicates positive part of the argument. The Eq. (3.1) encompasses three types of DFs based on the sign of the shape parameter, ζ: Fréchet ($\zeta > 0$), Weibull ($\zeta < 0$) and the Gumbel ($\zeta \to 0$). GEV distribution is a combination of Gumbel, Fréchet and Weibull distributions and is fitted to block or AM time series (Cheng and AghaKouchak, 2014; Katz et al., 2002; Katz and Brown, 1992). The GEV distribution contains three parameters, the location, the scale and the shape of the distribution, which describes the center of the distribution, the deviation around the mean and the shape or the tail of the distribution. The shape parameter, ζ zero indicates Gumbel, which is described by an unbounded light tailed distribution and the tail decreases rapidly following an exponential decay [*Markose and Alentorn*, 2011]. On the other hand, the positive shape parameter denotes Fréchet and is a heavy-tailed distribution, and the tail drops relatively slowly following a polynomial decay (Towler et al., 2010). The negative shape parameter represents a Weibull distribution, which is a bounded distribution.

SI 3.1 GEV Distribution with Time Varying Parameters

We assume the location and the scale parameters of the GEV distribution is linear function of time, while we kept shape parameter as constant:

$$\mu(t) = \mu_1 t + \mu_0 \tag{3.2}$$

$$\sigma(t) = \sigma_1 t + \sigma_0 \tag{3.3}$$

Since the scale parameter must be positive throughout, it is often modeled using a log link function (Gilleland and Katz, 2014)

$$\ln\sigma(t) = \sigma_1 t + \sigma_0 \;\Rightarrow\; \sigma(t) = \exp(\sigma_1 t + \sigma_0) \tag{3.4}$$

Where *t* is the time (in years), $\boldsymbol{\lambda} = \{\mu_1, \mu_0, \sigma_1, \sigma_0, \zeta\}$ are the parameters.

SI 3.2 Estimation of GEV Parameters

GEV parameters are estimated using (i) Maximum likelihood (ML) method and (ii) Bayesian Inference. For method (i) let $z_1,....,z_m$ represent the block maxima of samples of *m* blocks of length *n*, the log-likelihood for the stationary GEV DF is (Gilleland and Katz, 2014):

$$l\left(\mu,\sigma,\zeta;z_1,....,z_m\right)=-m\ln\sigma-\left(1+\left(1/\zeta\right)\right)\sum_{i=1}^{m}\ln\left[1+\zeta\left(\frac{z_i-\mu}{\sigma}\right)\right]_+-\sum_{i=1}^{m}\ln\left[1+\zeta\left(\frac{z_i-\mu}{\sigma}\right)\right]_+^{1/\zeta} \tag{3.5}$$

In this study, ML is implemented using MATLAB function 'gevfit' available in MATLAB statistical toolbox (in MATLAB R2016a platform).

For method (ii) a Bayesian analysis is performed by imposing a prior distribution on the parameters. We estimated parameters using Bayesian inference (BI) coupled with Differential Evaluation Markov Chain (DE-MC) simulation as in [*Cheng and AghaKouchak*, 2014; *Cheng et al.*, 2014]. This approach combines knowledge from a prior distribution and the observation vector $\boldsymbol{y}=\left\{y_t\right\}_{t=1:N}$ (*i.e.*, annual maxima rainfall) into the posterior distribution of parameters $\boldsymbol{\omega}=\left\{\mu,\sigma,\zeta\right\}$, where *N* denotes the number of annual maxima in the observation vector $\boldsymbol{Y}$. The Bayes theorem for estimation of GEV parameters under stationarity assumption can be expressed as (Cheng et al., 2014; Renard et al., 2013)

$$p(\boldsymbol{\omega}|\boldsymbol{y})\propto p(\boldsymbol{y}|\boldsymbol{\omega})p(\boldsymbol{\omega})=\prod_{t=1}^{N}p(\boldsymbol{y}|\boldsymbol{\omega})p(\boldsymbol{\omega}) \tag{3.6}$$

Under the assumption of nonstationarity, the equation (3.6) is given as (Cheng et al., 2014; Renard et al., 2013),

$$p(\boldsymbol{\lambda}|\boldsymbol{y},\boldsymbol{x})\propto p(\boldsymbol{y}|\boldsymbol{\lambda},\boldsymbol{x})p(\boldsymbol{\lambda}|\boldsymbol{x}) \tag{3.7}$$

$$p(\boldsymbol{y}|\boldsymbol{\lambda},\boldsymbol{x})=\prod_{t=1}^{N}p\left(\boldsymbol{y}_t|\boldsymbol{\omega},\boldsymbol{x}(t)\right)=\prod_{t=1}^{N}p\left(\boldsymbol{y}_t|\mu(t),\sigma(t),\zeta\right) \tag{3.8}$$

Where, $\boldsymbol{x}(t)$ denote covariates under nonstationarity. The posterior distributions, $p(\boldsymbol{\omega}|\boldsymbol{y})$ and $p(\boldsymbol{y}|\boldsymbol{\lambda},\boldsymbol{x})$ provide information about parameters under the assumption of stationarity, $\boldsymbol{\omega}=\left\{\mu,\sigma,\zeta\right\}$ and nonstationarity, $\boldsymbol{\lambda}=\left\{\mu_1,\mu_0,\sigma_1,\sigma_0,\zeta\right\}$ respectively. Since the posterior distributions of model parameters are, in general, analytically intractable, the DE-MC is integrated

with BI to generate a large number of realizations from parameters' posterior distributions [*Cheng et al.*, 2014]. DE-MC is an adaptive Monte Carlo Markov Chain (MCMC) algorithm (ter Braak and Vrugt, 2008; Ter Braak, 2006), in which multiple chains (here, we fix chain length '*n*' as 5) are run in parallel. The resulting MC simulation can then run to an equilibrium (often referred to as the *burn-in* period). It is a standard practice to discard the initial iterations of simulated samples since they are strongly influenced by starting values and do not provide usable information of the target distribution. Here we run DE-MC simulations for 3000 iterations and kept the iterations 2001-3000 of each chain. The convergence of MC simulation is checked by the "potential scale reduction factor ($\widehat{R}$)" as in (Gelman et al., 2011), which suggests the value of $\hat{R}$ should remain below the threshold value of 1.1. The post burn-in random draws from posterior distribution is then used to construct predictive distributions. For annual maxima time series of each duration, the mean and associated bounds of time invariant parameters ($\mu(t), \sigma(t)$) are derived by computing 50th (the median), 5th and 95th (bounds) percentiles of post *burn-in* random draw (for example, 50th percentile of $\mu(t_1), \ldots, \mu(t_{100})$). The derived model parameters are then used to compute corresponding design rainfall quantiles at *T*-year return period. For more details of BI and parameter estimation by DE-MC simulation, interested readers are requested to refer (Gelman et al., 2014; Renard et al., 2013).

SI 4 Model Selection by Akaike Information Criterion (AIC) for Small Samples

The AIC (Akaike, 1974; Bozdogan, 2000) is defined as follows:

$$AIC(m) = n\log(MSE) + 2m \tag{4.1}$$

Where *n* is the number of observations, *m* denotes the number of fitted model parameters. *MSE* is the mean square error of the fitted distribution against empirical distribution, which is expressed as,

$$MSE = \frac{1}{n-m}\sum_{i=1}^{n}(O_i - F_i)^2 \tag{4.2}$$

Where O_i and F_i are empirical (observed) and estimated distributions. The observed distribution (O_X) is computed using rank-based Gringorten's plotting position formula (Yue, 2001)

$$O_X\left(X \le x_i\right) = \frac{i - 0.44}{n + 0.12} \qquad \forall i = 1, 2, ..., n \tag{4.3}$$

Where, *i* is the rank in ascending order and x_i is the i^{th} largest variate in a data series of size *n*.

The *AIC* for small sample version is given by (Hurvich and Tsai, 1995),

$$AIC(m) = AIC + \frac{2m(m+1)}{n - m - 1} \tag{4.4}$$

SI 5 Estimation of Design Storm Intensity (DSI)

The DSI q_p, often referred as *return level* in the literature is the expected value to be exceeded on an average once in every $1/p$ periods, where $1 - p$ is the specific probability associated with the quantile (Gilleland and Katz, 2014). We obtain the $1 - p$ (*i.e.*, non-exceedance probability of occurrence) quantile of the annual maximum rainfall fitted with stationary GEV distribution using following expression [*Coles and Tawn*, 1996]:

$$q_p = \mu + \frac{\sigma}{\zeta}\left[\left\{-\ln\left(1-p\right)\right\}^{-\zeta} - 1\right] \qquad \forall \zeta \neq 0 \tag{5.1}$$

Where, q_p is the DSI, associated with a $T = 1/(1-p)$ - year return period. The nonstationary design intensity is analogous to the standard stationary precipitation intensity with the exception of inclusion of time variant parameters (Eqns. 3.2 and 3.3) (Cheng et al., 2014)

$$q_p = \bar{\mu} + \frac{\bar{\sigma}}{\zeta}\left[\left\{-\ln\left(1-p\right)\right\}^{-\zeta} - 1\right] \qquad \forall \zeta \neq 0 \tag{5.2}$$

Where time-variant parameters, $\bar{\mu}$ and $\bar{\sigma}$ are derived by computing 50th, 5th and 95th percentiles of DE-MC sampled $\mu(t)$ and $\sigma(t)$ $\left(\left\{\mu(t_1), ..., \mu(t_n)\right\} \text{ and } \left\{\sigma(t_1), ..., \sigma(t_n)\right\}\right)$ respectively.

SI 6 Statistical Significance of Nonstationary versus Stationary DSI

The (statistically) significant differences in DSI is computed using standard z-statistics, which is given by (Madsen et al., 2009; Mikkelsen et al., 2005)

$$z = \frac{\hat{z}_T^{NonSta} - \hat{z}_T^{Sta}}{\sqrt{0.5\left(var\{\hat{z}_T^{NonSta}\} + var\{\hat{z}_T^{Sta}\}\right)}} \quad (6.1)$$

Where $\hat{z}_T^{NonSta}$ is the *T*-year DSI obtained from the best selected nonstationary model, $\hat{z}_T^{Sta}$ describes the same but with the best stationary model. The denominator indicates predictive uncertainty; $var\{\hat{z}_T^{NonSta}\}$ and $var\{\hat{z}_T^{Sta}\}$ are the estimated variance obtained from the *T*-year event estimates and associated confidence interval (*i.e.*, 5th, and 95th quantile). The z-statistic can be interpreted as statistically equivalent to quantiles of standard normal distribution, *i.e.*, z = ± 1.96 and ± 1.64 correspond to 5% and 10% significance levels. The null hypothesis of the test assumes the *T*-year event estimate obtained using the best fitted nonstationary model is significantly different from its best fitted stationary counterpart.

Table S5. Selected stations and their statistical properties for annual maxima time series of rainfall volume

Stations	EC-Station ID	Analysis Period	Time Frame (min)	Mean (mm)	Std. deviation (mm)	Skew	Excess[1] Kurtosis
Toronto Int'l. Airport	6158731	1950 - 2013	15	16.35	5.88	0.46	-0.36
			30	21.85	8.68	0.86	0.9
Hamilton Airport	6153194	1960 - 2010	15	16.12	5.61	1.26	1.11
			30	16.63	8.47	4.45	24.09
Oshawa WPCP	6155878	1970 - 2015	15	56.01	17.84	0.84	1.68
			30	36.09	11.40	0.22	-0.57
Windsor Airport	6139525	1950 - 2013	15	17.79	5.56	1.03	1.69
			30	23.49	8.20	0.77	-0.15
Kingston P. Station	6104175	1961 - 2007	15	12.89	3.79	0.93	2.15
			30	16.54	5.31	0.78	1.12
London Airport	6144478/75*	1950 – 2015	15	15.96	6.62	1.28	1.73
			30	21.06	8.55	1.68	3.94
Trenton Airport	6158875	1950 – 2015	15	13.30	6.52	2.90	10.23
			30	16.60	6.40	1.54	2.97
Stratford WWTP	6148100	1960 – 2015	15	16.33	5.08	1.30	2.23
			30	21.37	9.08	2.22	7.53
Fergus Shand Dam	6142400	1950 – 2015	15	17.74	6.66	1.24	2.14
			30	23.42	10.32	1.78	4.04

*Missing values are infilled using observations from the nearest station ID 6144475.[1]Kurtosis relative to normal distribution, *i.e.*, kurtosis – 3.

Table S6. Selected stations and their statistical properties for hourly annual maxima rainfall volume for selected durations

Stations	EC-Station ID	Analysis Period	Time Frame (hr)	Mean	Std. Deviation (mm)	Skew	Excess Kurtosis
Toronto Int'l. Airport	6158731	1950 - 2013	1	24.67	11.01	1.98	7.33
			6	38.44	18.09	2.46	7.93
Hamilton Airport	6153194	1960 - 2010	1	25.91	10.30	2.54	10.20
			6	38.72	15.05	2.34	7.07
Oshawa WPCP	6155878	1970 - 2015	1	22.09	8.56	0.54	-0.43
			6	5.94	2.05	1.18	0.99
Windsor Airport	6139525	1950 - 2013	1	29.53	10.43	0.88	0.14
			6	44.36	14.81	1.12	1.81
Kingston P. Station	6104175	1961 - 2007	1	21.21	6.83	0.56	-0.03
			6	37.35	13.61	2.32	8.05
London Airport	6144478/75	1950 – 2015	1	24.26	11.23	2.41	9.79
			6	36.46	12.10	1.73	4.57
Trenton Airport	6158875	1950 – 2015	1	20.36	8.25	1.87	6.03
			6	36.76	12.51	1.19	0.66
Stratford WWTP	6148100	1960 – 2015	1	24.31	11.12	1.71	3.41
			6	41.77	21.61	2.31	6.15
Fergus Shand Dam	6142400	1950 – 2015	1	28.07	13.67	2.02	5.50
			6	39.86	18.59	1.25	2.30

Table S7. Detection of trends and nonstationarity in Toronto Pearson International Airport

Time Slice	Ljung-Box Test	Augmented Dickey-Fuller Test		KPSS Test		Mann-Kendall Trend Test			Priestley-Subbarao Test	Pettitt Test	Mann-Whitney Change Point Test			Mood Change Point Test		
	p-value	Test statistics	p-value	Test statistics	p-value	MK_Z	β	p-value	p-value	p-value	Year	Test statistics	Threshold	Year	Test statistics	Threshold
15-min	0.014**	-0.326	0.53**	0.120	0.098*	-0.71	-0.23	0.48	0.383	0.141	x	x	x	x	x	x
30-min	0.027**	-0.177	0.58**	0.123	0.092*	-0.52	-0.25	0.61	0.283	0.179	x	x	x	x	x	x
1-hr	0.805	-0.077	0.62**	0.138	0.064*	0.39	0.22	0.69	0.409	0.368	x	x	x	x	x	x
2-hr	0.920	0.043	0.66**	0.129	0.081*	-0.07	-0.05	0.94	0.143	0.564	x	x	x	x	x	x
6-hr	0.959	0.051	0.67**	0.060	> 0.10	-0.61	-0.48	0.54	0.025	0.733	x	x	x	x	x	x
12-hr	0.965	0.106	0.67**	0.065	> 0.10	-0.55	-0.49	0.58	$2.0e^{-4}$**	0.659	x	x	x	x	x	x
24-hr	0.885	0.106	0.69**	0.046	> 0.10	-0.06	-0.06	0.95	0.046**	1.221	x	x	x	x	x	x

** and * indicate statistically significant at 5% and 10% significance levels, 'x' denotes no change points detected using Mann-Whitney and Mood tests respectively. β indicates slope per decade calculated using Theil-Sen method. *P-values* larger than 0.1 in KPSS test indicates test statistics are non-significant, whereas *p-values* smaller than 0.01 are considered to be highly significant. The standardized Mann-Kendall test statistic (MK_Z) is positive (negative) with an increasing (decreasing) trend, and statistically significant at 5% and 10% significance levels when $|MK_Z| > 1.96$ and $|MK_Z| > 1.64$ respectively. Change point tests are performed at 10% significance level.

Table S7.1 Detection of trends and nonstationarity after performing TFPW in Toronto Pearson International Airport

Time Slice	Ljung-Box Test	Augmented Dickey-Fuller Test		KPSS Test		Mann-Kendall Trend Test			Priestley-Subbarao Test	Pettitt Test	Mann-Whitney Change Point Test			Mood Change Point Test		
	p-value	Test statistics	p-value	Test statistics	p-value	MK_Z	β	p-value	p-value	p-value	Year	Test statistics	Threshold	Year	Test statistics	Threshold
15-min	0.258	-0.60**	0.43	0.089	>0.10	-0.17	-0.04	0.87	0.504	0.531	x	x	x	x	x	x
30-min	0.243	-0.35**	0.52	0.098	>0.10	0.07	0.05	0.94	0.498	0.777	x	x	x	x	x	x

Table S8. Detection of trends and nonstationarity in Hamilton Airport

Time Slice	Ljung-Box Test	Augmented Dickey-Fuller Test		KPSS Test		Mann-Kendall Trend Test			Priestley-Subbarao Test	Pettitt Test	Mann-Whitney Change Point Test			Mood Change Point Test		
	p-value	Test statistics	p-value	Test statistics	p-value	MK_Z	β	p-value	p-value	p-value	Year	Test statistics	Threshold	Year	Test statistics	Threshold
15-min	0.173	-0.454	0.48**	0.033	>0.10	-0.65	-0.24	0.516	0.406	0.438	x	x	x	x	x	x
30-min	0.911	-0.428	0.49**	0.047	>0.10	-1.186	-0.45	0.236	2.56e-5**	0.402	x	x	x	x	x	x
1-hr	0.918	-0.170	0.58**	0.082	>0.10	0.244	0.28	0.807	0.002**	0.870	x	x	x	x	x	x
2-hr	0.735	-0.176	0.58**	0.154	0.043**	1.023	0.75	0.306	8.03e-6**	0.300	x	x	x	x	x	x
6-hr	0.099*	-0.138	0.60**	0.193	0.019**	-0.097	-0.11	0.922	3.49e-9**	0.216	x	x	x	x	x	x
12-hr	0.150	-0.055	0.63**	0.183	0.023**	-0.122	-0.14	0.903	2.78e-10**	0.506	x	x	x	x	x	x
24-hr	0.059*	-0.035	0.63**	0.307	0.010**	0.309	0.39	0.758	1.82e-7**	0.199	x	x	x	x	x	x

Table S8.1 Detection of trends and nonstationarity after performing TFPW in Hamilton Airport

Time Slice	Ljung-Box Test	Augmented Dickey-Fuller Test		KPSS Test		Mann-Kendall Trend Test			Priestley-Subbarao Test	Pettitt Test	Mann-Whitney Change Point Test			Mood Change Point Test		
	p-value	Test statistics	p-value	Test statistics	p-value	MK_Z	β	p-value	p-value	p-value	Year	Test statistics	Threshold	Year	Test statistics	Threshold
6-hr	0.108	-0.211	0.570**	0.197	0.02**	-0.02	-0.03	0.981	2.83e-6**	0.227	x	x	x	x	x	x
24-hr	0.282	-0.202	0.573**	0.282	0.01**	0.318	0.41	0.751	9.78e-4**	0.316	x	x	x	x	x	x

Table S9. Detection of trends and nonstationarity in Oshawa WPCP

Time Slice	Ljung-Box Test	Augmented Dickey-Fuller Test		KPSS Test		Mann-Kendall Trend Test			Priestley-Subbarao Test	Pettitt Test	Mann-Whitney Change Point Test			Mood Change Point Test		
	p-value	Test statistics	p-value	Test statistics	p-value	MK_Z	β	p-value	p-value	p-value	Year	Test statistics	Threshold	Year	Test statistics	Threshold
15-min	0.986	-0.152	0.59**	0.044	>0.10	0.93	2.12	0.35	0.18	0.89	x	x	x	x	x	x
30-min	0.620	-0.251	0.55**	0.045	>0.10	0.73	1.02	0.47	0.92	1.094	x	x	x	1974	2.62*	2.59
1-hr	0.994	-0.065	0.62**	0.081	>0.10	1.29	1.5	0.20	0.57	0.562	x	x	x	x	x	x
2-hr	0.938	-0.116	0.61**	0.08	>0.10	1.68	0.82	0.09*	0.005**	0.259	2009	2.64*	2.58	x	x	x
6-hr	0.924	-0.311	0.53**	0.075	>0.10	1.49	0.3	0.14	0.027**	0.248	x	x	x	x	x	x
12-hr	0.998	-0.928	0.31**	0.048	>0.10	1.73	0.13	0.08*	$2.4e^{-4}$**	0.321	1975	2.59*	2.67	x	x	x
24-hr	0.990	-1.716	0.08*	0.040	>0.10	2.20	0.14	0.03**	$2.4e^{-3}$**	0.056*	1983	2.90*	2.58	x	x	x

Table S10. Detection of trends and nonstationarity in Windsor Airport

Time Slice	**Ljung-Box Test**	**Augmented Dickey-Fuller Test**		**KPSS Test**		**Mann-Kendall Trend Test**		**Priestley-Subbarao Test**	**Pettitt Test**	**Mann-Whitney Change Point Test**			**Mood Change Point Test**		
	p-value	Test statistics	p-value	Test statistics	p-value	MK_Z	β	p-value	p-value	Year	Test statistics	Threshold	Year	Test statistics	Threshold
15-min	0.595	-0.237	0.56**	0.108	>0.10	-1.29	-0.42	0.198	0.156	0.141	x	x	x	x	x	x
30-min	0.749	-0.363	0.51**	0.074	>0.10	-1.59	-0.77	0.111	0.845	0.093*	x	x	x	x	x	x
1-hr	0.462	-0.366	0.51**	0.083	>0.10	-1.52	-0.9	0.129	0.851	0.103	x	x	x	x	x	x
2-hr	0.614	-0.222	0.56**	0.127	0.085*	-0.82	-0.74	0.414	0.529	0.281	2005	2.99*	2.63	x	x	x
6-hr	0.504	-0.098	0.61**	0.128	0.084*	-0.47	-0.45	0.656	0.256	0.300	2005	2.95*	2.63	x	x	x
12-hr	0.969	-0.238	0.56**	0.065	>0.10	-1.48	-1.4	0.138	0.296	0.141	x	x	x	x	x	x
24-hr	0.414	-0.177	0.58**	0.041	>0.10	-0.035	-0.01	0.972	0.976	0.940	x	x	x	x	x	x

Table S11. Detection of trends and nonstationarity in Kingston P. Station

Time Slice	**Ljung-Box Test**	**Augmented Dickey-Fuller Test**		**KPSS Test**		**Mann-Kendall Trend Test**			**Priestley-Subbarao Test**	**Pettitt Test**	**Mann-Whitney Change Point Test**			**Mood Change Point Test**		
	p-value	Test statistics	p-value	Test statistics	p-value	MK_Z	β	p-value	p-value	p-value	Year	Test statistics	Threshold	Year	Test statistics	Threshold
15-min	0.257	-0.502	0.46**	0.024	>0.10	0.63	0.2	0.53	0.040	1.38	x	x	x	x	x	x
30-min	0.094	-0.485	0.47**	0.027	>0.10	0.18	0.12	0.85	0.322	1.59	x	x	x	x	x	x
1-hr	0.371	-0.316	0.53**	0.039	>0.10	0.16	0.12	0.88	0.094*	1.10	x	x	x	1996	2.73*	2.6
2-hr	0.124	-0.306	0.53**	0.084	>0.10	0.05	0.03	0.96	0.333	1.06	x	x	x	x	x	x
6-hr	0.273	-0.330	0.53**	0.168	0.032**	-0.22	-0.36	0.83	0.0009**	0.397	x	x	x	x	x	x
12-hr	0.886	-0.298	0.54**	0.102	>0.10	0.56	0.39	0.58	5.53e-6**	0.347	x	x	x	x	x	x
24-hr	0.346	-0.258	0.55**	0.131	0.078*	0.68	0.75	0.50	1.06e-5**	0.514	1965	2.62*	2.60	x	x	x

Table S12. Detection of trends and nonstationarity in London International Airport

Time Slice	Ljung-Box Test	Augmented Dickey-Fuller Test		KPSS Test		Mann-Kendall Trend Test			Priestley-Subbarao Test	Pettitt Test	Mann-Whitney Change Point Test			Mood Change Point Test		
	p-value	Test statistics	p-value	Test statistics	p-value	MK_Z	β	p-value	p-value	p-value	Year	Test statistics	Threshold	Year	Test statistics	Threshold
15-min	0.344	-0.662	0.41**	0.179	0.024**	-0.549	-0.23	0.583	0.092*	0.253	2006	2.94*	2.63	2006	3.09*	2.66
30-min	0.288	-0.598	0.43**	0.106	>0.10	-1.422	-0.64	0.155	0.019**	0.240	2005	2.87*	2.63	x	x	x
1-hr	0.783	-0.487	0.47**	0.117	>0.10	-1.173	-0.66	0.241	0.031**	0.359	2011	3.06*	2.63	2011	2.96*	2.66
2-hr	0.845	-0.552	0.45**	0.135	0.070*	-1.566	-1.03	0.117	0.224	0.216	2011	3.14*	2.63	2011	3.15*	2.66
6-hr	0.700	-0.418	0.49**	0.071	>0.10	-1.893	-1.11	0.058*	0.199	0.161	2011	3.01*	2.63	2011	2.80*	2.66
12-hr	0.587	-0.347	0.52**	0.090	>0.10	-2.142	-1.47	0.032**	0.755	0.093*	2011	2.98*	2.63	x	x	x
24-hr	0.733	-0.414	0.50**	0.223	0.010**	-2.297	-2.45	0.022**	0.909	0.024**	2005	3.46*	2.63	x	x	x

Table S13. Detection of trends and nonstationarity in Trenton Airport

Time Slice	Ljung-Box Test	Augmented Dickey-Fuller Test		KPSS Test		Mann-Kendall Trend Test			Priestley-Subbarao Test	Pettitt Test	Mann-Whitney Change Point Test			Mood Change Point Test		
	p-value	Test statistics	p-value	Test statistics	p-value	MK_Z	β	p-value	p-value	p-value	Year	Test statistics	Threshold	Year	Test statistics	Threshold
15-min	0.263	-0.398	0.50**	0.051	>0.10	0.708	0.16	0.479	2.65e-6**	0.893	x	x	x	1979	3.66*	2.66
30-min	0.161	-0.325	0.53**	0.034	>0.10	1.732	0.68	0.083*	0.0033**	0.264	x	x	x	1978	3.16*	2.66
1-hr	0.373	-0.328	0.53**	0.061	>0.10	1.776	0.87	0.076*	0.0013**	0.098*	x	x	x	x	x	x
2-hr	0.423	-0.341	0.52**	0.063	>0.10	2.313	1.27	0.021**	5.1e-5**	0.053*	1994	2.81*	2.63	x	x	x
6-hr	0.638	-0.244	0.56**	0.078	>0.10	2.031	1.12	0.042**	0.005**	0.092*	1994	2.66*	2.63	x	x	x
12-hr	0.295	-0.105	0.61**	0.204	0.014**	2.009	1.64	0.045**	0.044**	0.022**	1996	3.25*	2.63	x	x	x
24-hr	0.321	-0.131	0.60**	0.238	0.010**	2.031	1.82	0.042**	0.39	0.014**	1994	3.37*	2.63	x	x	x

Table S14. Detection of trends and nonstationarity in Stratford WWTP

Time Slice	**Ljung-Box Test**	**Augmented Dickey-Fuller Test**		**KPSS Test**		**Mann-Kendall Trend Test**			**Priestley-Subbarao Test**	**Pettitt Test**	**Mann-Whitney Change Point Test**			**Mood Change Point Test**		
	p-value	Test statistics	p-value	Test statistics	p-value	MK_Z	β	p-value	p-value	p-value	Year	Test statistics	Threshold	Year	Test statistics	Threshold
15-min	0.070	-0.321	0.53**	0.068	>0.10	-0.233	-0.07	0.816	0.143	1.19	1994	3.37*	2.63	x	x	x
30-min	0.473	-0.375	0.51**	0.039	>0.10	-0.297	-0.13	0.767	0.004**	1.44	x	x	x	2011	3.23*	2.63
1-hr	0.857	-0.230	0.56**	0.077	>0.10	0.417	0.26	0.677	0.013**	1.01	x	x	x	x	x	x
2-hr	0.149	-0.263	0.55**	0.055	>0.10	0.389	0.3	0.697	0.016**	1.14	x	x	x	1967	2.73*	2.63
6-hr	0.375	-0.134	0.60**	0.062	>0.10	-0.459	-0.51	0.646	$3.9e^{-4}$**	0.802	x	x	x	x	x	x
12-hr	0.336	-0.186	0.58**	0.058	>0.10	0.82	-0.67	0.412	$8.9e^{-5}$**	0.254	x	x	x	x	x	x
24-hr	0.789	-0.208	0.57**	0.056	>0.10	-1.442	-1.43	0.149	$8.7e^{-4}$**	0.360	x	x	x	x	x	x

Table S15. Detection of trends and nonstationarity in Fergus Shand Dam

Time Slice	Ljung-Box Test	Augmented Dickey-Fuller Test		KPSS Test		Mann-Kendall Trend Test			Priestley-Subbarao Test	Pettitt Test	Mann-Whitney Change Point Test			Mood Change Point Test		
	p-value	Test statistics	p-value	Test statistics	p-value	MK_Z	β	p-value	p-value	p-value	Year	Test statistics	Threshold	Year	Test statistics	Threshold
15-min	0.955	-0.267	0.550	0.184	0.022**	-0.99	-0.43	0.322	0.049**	0.25	x	x	x	x	x	x
30-min	0.935	-0.204	0.573	0.172	0.028**	-0.44	-0.27	0.658	0.015**	0.33	x	x	x	x	x	x
1-hr	0.879	-0.494	0.467	0.068	>0.10	-1.00	-0.72	0.317	0.004**	0.57	x	x	x	x	x	x
2-hr	0.849	-0.540	0.450	0.055	>0.10	-0.92	-0.69	0.358	0.002**	0.67	x	x	x	x	x	x
6-hr	0.967	-0.318	0.532	0.104	>0.10	-0.26	-0.29	0.795	0.053**	0.77	x	x	x	x	x	x
12-hr	0.018** (0.033**)	-0.116	0.606	0.035	>0.10	-0.45	-0.28	0.652	0.255	1.12	x	x	x	x	x	x
24-hr	1.5e-4** (0.011**)	-0.218	0.568	0.035	>0.10	-1.34	-1.2	0.180	0.216	0.53	x	x	x	x	x	x

[1]Values within first Brackets indicate p-values of Ljung-Box Test after performing two-successive TFPWs.

Table S16. Performance of stationary and nonstationary models for Toronto Pearson International Airport

Time Slice	Model	Location parameter	Scale parameter	Shape parameter	AIC_c	LB (100yr)	UB (100yr)	UB/LB
15-min	GEV_0-ML	31.86	15.77	-0.30	-451.49	92.53	158.7	1.72
	GEV_0-DEMC	37.45	19.98	-0.10	***-459.11***	78.85	201.07	2.55
	GEV_t-I	35.13 + 0.062*t*	17.96	-0.033	-440.42	88.96	158.46	1.78
	GEV_t-II	37.055 – 0.0024*t*	exp(3.02 – 0.0015*t*)	-0.11	**-443.72**	91.21	129.93	1.42
30-min	GEV_0-ML	21.80	10.56	-0.184	-437.81	69.93	135.02	1.93
	GEV_0-DEMC	25.43	13.29	0.015	***-439.97***	63.56	134.98	2.12
	GEV_t-I	25.98 – 0.0041*t*	13.65	-0.038	-437.93	69.34	101.21	1.46
	GEV_t-II	26.31 – 0.032*t*	exp(2.58 – 2.0e^{-5}*t*)	0.027	**-439.67**	65.86	117.76	1.79
1-hr	GEV_0-ML	17.70	6.32	-0.11	***-480.40***	49.34	90.15	1.83
	GEV_0-DEMC	19.49	7.92	0.067	-464.17	46.84	90.37	1.93
	GEV_t-I	17.62 + 0.059*t*	8.54	0.052	-453.83	48.65	98.42	2.02
	GEV_t-II	17.62 + 0.071*t*	exp(1.81 – 0.0075*t*)	0.06	**-482.50**	55.16	68.77	1.25
2-hr	GEV_0-ML	10.46	3.41	-0.047	-486.91	29.75	59.29	1.99
	GEV_0-DEMC	11.80	4.16	0.11	***-491.95***	27.77	51.71	1.86
	GEV_t-I	11.55 + 0.0004*t*	4.30	0.19	-475.28	35.86	50.81	1.42
	GEV_t-II	10.99 + 0.02*t*	exp(1.31 + 0.0044*t*)	0.16	**-476.78**	34.91	46.66	1.34
6-hr	GEV_0-ML	4.58	1.18	0.05	**-503.95**	13.47	39.04	2.90
	GEV_0-DEMC	5.04	1.49	0.25	-499.82	13.02	29.43	2.26
	GEV_t-I	5.20 -0.0042*t*	1.56	0.27	***-511.36***	16.23	22.39	1.38
	GEV_t-II	3.02 – 0.0026*t*	exp(-0.42 + 0.00069*t*)	0.43	-502.03	10.94	14.93	1.36
12-hr	GEV_0-ML	2.75	0.53	0.14	**-526.12**	7.94	30.49	3.84
	GEV_0-DEMC	3.01	0.77	0.32	-520.52	7.97	20.19	2.53
	GEV_t-I	3.03 – 0.003*t*	0.70	0.43	***-541.11***	10.23	16.8	1.64
	GEV_t-II	0.46 – 0.0036*t*	exp(3.28-0.0039*t*)	-0.32	-517.21	10.88	16.15	1.48
24-hr	GEV_0-ML	1.59	0.32	0.10	***-479.66***	4.18	11.3	2.70
	GEV_0-DEMC	1.71	0.40	0.29	-471.58	4.03	9.15	2.27
	GEV_t-I	1.71 -0.0006*t*	0.41	0.30	-469.76	4.11	7.92	1.93
	GEV_t-II	1.71 + 0.0003*t*	exp(-0.86+0.00085*t*)	0.26	**-474.07**	4.48	8.3	1.85

* GEV_0-ML, GEV_0-DEMC are stationary models whereas GEV_t-I and GEV_t-II are nonstationary models with time-variant mean, and both time-variant mean and standard deviation respectively. ML denotes parameter estimated using Maximum Likelihood (ML) method and DEMC denotes GEV parameters estimated by coupling BI with DE-MC simulation. The best fitted stationary model is marked in bold italics in blue and the best nonstationary model is shown in red and bold letters. LB and UB indicates lower and upper bound of DSI at 100-year return period.

Table S17. Performance of stationary and nonstationary models for Hamilton Airport

Time Slice	Model	Location parameter	Scale parameter	Shape parameter	AIC_c	LB (100yr)	UB (100yr)	UB/LB
15-min	GEV_0-ML	49.12	11.36	-0.078	***-350.91***	114.98	269.92	2.35
	GEV_0-DEMC	53.09	13.82	0.14	-328.77	107.19	142.58	1.33
	GEV_t-I	55.54-0.017*t*	16.03	0.023	**-326.49**	107.3	172.18	1.60
	GEV_t-II	59.94-0.21*t*	exp(3.31-0.017*t*)	0.112	-326.73	132.38	190.73	1.44
30-min	GEV_0-ML	24.82	5.52	0.024	***-372.80***	62.26	147.67	2.37
	GEV_0-DEMC	26.86	7.16	0.20	-368.33	59.53	124.5	2.09
	GEV_t-I	28.30-0.04*t*	7.33	0.11	**-367.50**	60.96	85.66	1.41
	GEV_t-II	28.10-0.04*t*	exp(2.16-0.007*t*)	0.11	-366.89	58.38	90.22	1.55
1-hr	GEV_0-ML	19.45	4.96	-0.080	-356.63	47.65	104.07	2.18
	GEV_0-DEMC	21.45	6.33	0.122	***-368.33***	43.48	87.78	2.02
	GEV_t-I	21.38+0.0054*t*	6.55	0.057	**-357.33**	48.87	64.98	1.33
	GEV_t-II	24.18+0.14*t*	exp(1.96+0.015*t*)	0.033	-353.97	46.83	65.05	1.39
2-hr	GEV_0-ML	11.60	2.88	-0.049	***-356.95***	27.39	49.43	1.80
	GEV_0-DEMC	12.78	3.67	0.11	-351.85	26.9	50.6	1.88
	GEV_t-I	12.49+0.011*t*	3.71	0.05	**-355.41**	27.2	37.41	1.38
	GEV_t-II	12.48+0.0047*t*	exp(1.42-0.0013*t*)	0.19	-318.74	36.28	49.73	1.37
6-hr	GEV_0-ML	4.84	0.956	0.03	***-393.86***	12.14	39.66	3.27
	GEV_0-DEMC	5.21	1.21	0.29	-372.63	10.47	33.52	3.20
	GEV_t-I	5.11+0.003*t*	1.28	0.34	-405.31	16.01	24.51	1.53
	GEV_t-II	5.10+0.0043*t*	exp(0.30-0.0020*t*)	0.34	**-407.78**	14.3	26.45	1.85
12-hr	GEV_0-ML	2.88	0.569	-0.01	***-371.91***	6.63	16.58	2.50
	GEV_0-DEMC	3.12	0.75	0.18	-369.72	5.91	15.07	2.55
	GEV_t-I	3.01+0.003*t*	0.75	0.24	**-371.40**	8	11.54	1.44
	GEV_t-II	3.17+0.002*t*	exp(-0.28+0.002*t*)	0.04	-331.06	6.25	8.89	1.42
24-hr	GEV_0-ML	1.27	0.365	-0.06	-334.64	3.55	10.18	2.87
	GEV_0-DEMC	1.45	0.492	0.19	***-338.54***	3.47	5.06	1.46
	GEV_t-I	1.34+0.0041*t*	0.490	0.19	**-340.40**	4.26	6.12	1.44
	GEV_t-II	1.34+0.0033*t*	exp(-0.74 + 0.0003*t*)	0.19	-337.35	3.55	7.96	2.24

Table S18. Performance of stationary and nonstationary models for Oshawa WPCP

Time Slice	Model	Location parameter	Scale parameter	Shape parameter	AIC_c	LB (100yr)	UB (100yr)	UB/LB
15-min	GEV_0-ML	43.69	12.35	-0.24	***-336.05***	93.31	142.12	1.52
	GEV_0-DEMC	48.39	15.67	-0.074	-333.53	86.59	145.88	1.68
	GEV_t-I	44.87+0.22*t*	18.08	-0.13	**-289.90**	82.05	181.17	2.21
	GEV_t-II	38.83+0.29*t*	exp(2.67+0.0094*t*)	0.25	-237.45	135.57	295.37	2.18
30-min	GEV_0-ML	28.32	8.48	-0.46	-301.17	56.47	83.56	1.48
	GEV_0-DEMC	31.83	10.74	-0.20	***-305.98***	49.33	94.73	1.92
	GEV_t-I	29.1 + 0.105*t*	10.46	-0.16	**-304.85**	52.45	87.55	1.67
	GEV_t-II	29.53+0.12*t*	exp(2.37+0.0016*t*)	-0.28	-300.82	53.05	72.22	1.36
1-hr	GEV_0-ML	15.91	5.53	-0.34	-309.56	38.66	81.13	2.10
	GEV_0-DEMC	18.45	7.18	-0.01	***-327.32***	34.31	82.16	2.39
	GEV_t-I	16.32 + 0.07*t*	7.09	0.008	**-311.38**	43.9	60.67	1.38
	GEV_t-II	8.94+0.35*t*	exp(1.84+0.011*t*)	0.14	-275.75	42.15	170.26	4.04
2-hr	GEV_0-ML	9.83	2.76	-0.12	-320.35	25.63	70.31	2.74
	GEV_0-DEMC	11.28	3.70	0.12	***-328.90***	23.02	63.23	2.75
	GEV_t-I	10.03+0.043*t*	3.71	0.13	-325.83	27.98	43.76	1.56
	GEV_t-II	10.38+0.039*t*	exp(1.31+0.002*t*)	0.18	**-331.75**	34.23	46.94	1.37
6-hr	GEV_0-ML	4.53	1.12	-0.13	-312.53	10.31	21.33	2.07
	GEV_0-DEMC	5.03	1.47	0.08	***-313.6***	9.55	20.76	2.17
	GEV_t-I	4.46+0.02*t*	1.42	0.10	-318.20	11.45	15.79	1.38
	GEV_t-II	4.11+0.03*t*	exp(0.127+0.008*t*)	0.14	**-319.01**	11.75	16.46	1.40
12-hr	GEV_0-ML	2.60	0.57	0.086	***-317.28***	7.16	21.84	3.05
	GEV_0-DEMC	2.82	0.78	0.29	-310.19	6.82	17.52	2.57
	GEV_t-I	2.74+0.0067*t*	0.78	0.31	**-317.51**	9.23	12.8	1.39
	GEV_t-II	2.65+0.0098*t*	exp(-0.27+0.0031*t*)	0.32	-315.25	9.87	13.45	1.36
24-hr	GEV_0-ML	1.48	0.38	-0.048	***-317.60***	3.79	9.14	2.41
	GEV_0-DEMC	1.67	0.50	0.14	-316.68	3.54	8.38	2.37
	GEV_t-I	1.52+0.006*t*	0.52	0.17	**-318.12**	4.51	6.26	1.39
	GEV_t-II	1.48+0.008*t*	exp(-0.69+0.0025*t*)	0.15	-314.06	3.84	8.6	2.24

Table S19. Performance of stationary and nonstationary models for Windsor Airport

Time Slice	Model	Location parameter	Scale parameter	Shape parameter	AIC_c	LB (100yr)	UB (100yr)	UB/LB
15-min	GEV_0-ML	55.0	11.94	-0.16	-388.88	123.47	345.02	2.79
	GEV_0-DEMC	60.0	15.72	0.13	***-393.03***	116.82	250.65	2.15
	GEV_t-I	64.23-0.11*t*	16.92	-0.009	**-395.46**	116.66	161.22	1.38
	GEV_t-II	62.26-0.14*t*	exp(2.95 – 0.0049*t*)	0.11	-395.27	122.45	210.63	1.72
30-min	GEV_0-ML	35.43	9.55	-0.16	-426.11	83.93	183.56	2.19
	GEV_0-DEMC	38.90	12.41	0.094	***-440.87***	76.91	182.68	2.38
	GEV_t-I	44.56-0.13*t*	13.80	-0.06	**-424.30**	81.03	118.95	1.47
	GEV_t-II	45.38-0.21*t*	exp(3.15-0.017*t*)	0.31	-416.35	127.28	250.39	1.97
1-hr	GEV_0-ML	22.49	6.35	-0.16	-452.06	52.5	96.42	1.84
	GEV_0-DEMC	24.79	7.99	0.03	***-455.42***	48.12	98.38	2.04
	GEV_t-I	28.60-0.13*t*	7.42	0.12	**-461.69**	60.04	82.68	1.38
	GEV_t-II	27.14-0.05*t*	exp(2.28-0.004*t*)	0.04	-422.03	54.11	94.36	1.74
2-hr	GEV_0-ML	14.14	4.26	-0.34	-469.94	29.07	41.45	1.43
	GEV_0-DEMC	15.60	5.25	-0.12	***-489.04***	25.78	46.21	1.79
	GEV_t-I	15.38-0.0085*t*	5.33	-0.12	-437.30	26.99	45.97	1.70
	GEV_t-II	17.42 – 0.056*t*	exp(1.62 + 0.002*t*)	-0.15	**-479.91**	30.18	36.75	1.22
6-hr	GEV_0-ML	5.74	1.51	-0.16	-472.61	12.9	23.06	1.79
	GEV_0-DEMC	6.25	1.91	0.041	***-479.53***	12.02	24.43	2.03
	GEV_t-I	6.93-0.02*t*	1.88	0.069	**-485.16**	14.24	18.52	1.30
	GEV_t-II	6.53-0.0093*t*	exp(0.53 + 0.003*t*)	0.093	-474.68	12.91	24.63	1.91
12-hr	GEV_0-ML	3.21	0.77	-0.12	-475.1	7.22	14.31	1.98
	GEV_0-DEMC	3.51	0.97	0.09	***-488.10***	6.61	13.97	2.11
	GEV_t-I	3.87 -0.011*t*	0.94	0.09	-475.93	7.81	10.4	1.33
	GEV_t-II	3.91 – 0.013*t*	exp(-0.10 + 0.0014*t*)	0.23	**-486.85**	9.72	13.01	1.34
24-hr	GEV_0-ML	1.87	0.43	-0.20	-461.41	3.8	6.67	1.76
	GEV_0-DEMC	2.03	0.55	0.03	***-486.47***	3.57	6.74	1.89
	GEV_t-I	2.069 - 0.0016*t*	0.54	0.005	-465.18	3.77	5.66	1.50
	GEV_t-II	2.07-0.002*t*	exp(-0.66+0.00085*t*)	0.057	**-483.82**	4.14	5.78	1.40

Table S20. Performance of stationary and nonstationary models for Kingston Airport

Time Slice	Model	Location parameter	Scale parameter	Shape parameter	AIC_c	LB (100yr)	UB (100yr)	UB/LB
15-min	GEV_0-ML	41.08	10.17	-0.24	-327.36	83.67	132.69	1.59
	GEV_0-DEMC	45.20	12.78	-0.041	***-329.1***	82.39	137.65	1.67
	GEV_t-I	41.11 + 0.17*t*	13.22	-0.045	**-320.65**	64.37	159.59	2.48
	GEV_t-II	37.16 + 0.34*t*	exp(2.78 – 0.0001*t*)	-0.22	-296.86	79.45	108.89	1.37
30-min	GEV_0-ML	25.68	7.15	-0.26	-344.91	55.1	90.24	1.64
	GEV_0-DEMC	28.84	8.92	-0.06	***-352.65***	51.14	87.88	1.72
	GEV_t-I	26.82 + 0.056*t*	9.20	-0.04	**-335.04**	50.77	100.47	1.98
	GEV_t-II	25.39 + 0.20*t*	exp(1.78 + 0.02*t*)	-0.14	-300.17	55.21	75.14	1.36
1-hr	GEV_0-ML	16.42	4.65	-0.32	***-321.42***	34.63	57.94	1.67
	GEV_0-DEMC	18.01	5.94	-0.06	-313.94	31.8	60.63	1.91
	GEV_t-I	15.28+0.094*t*	5.51	0.18	-286.73	45.94	72.49	1.58
	GEV_t-II	18.29+0.022*t*	exp(1.89-0.005*t*)	-0.13	**-321.01**	31.87	48.55	1.52
2-hr	GEV_0-ML	10.32	2.39	-0.21	***-323.34***	22.06	47.82	2.17
	GEV_0-DEMC	11.31	3.19	0.035	-322.59	20.65	41.49	2.01
	GEV_t-I	11.05+0.008*t*	3.14	0.008	**-324.96**	25.02	33.03	1.32
	GEV_t-II	11.27 + 0.0033*t*	exp(1.22 – 0.0045*t*)	0.031	-308.16	22.77	31.33	1.38
6-hr	GEV_0-ML	4.80	1.09	-0.06	***-330.38***	10.92	21.56	1.97
	GEV_0-DEMC	5.25	1.41	0.11	-330.16	10.3	21.51	2.09
	GEV_t-I	5.09 + 0.007*t*	1.41	0.14	**-333.51**	11.96	17.51	1.46
	GEV_t-II	5.18 + 0.002*t*	exp(0.322 – 0.0015*t*)	0.08	-317.98	9.97	16.48	1.65
12-hr	GEV_0-ML	2.84	0.64	-0.03	-322.32	6.54	12.83	1.96
	GEV_0-DEMC	3.08	0.80	0.17	***-326.52***	6.83	11.63	1.70
	GEV_t-I	2.84 + 0.011*t*	0.82	0.16	**-323.49**	6.55	11.67	1.78
	GEV_t-II	2.82 + 0.009*t*	exp(-0.22-0.0033*t*)	0.13	-316.56	6.02	9.93	1.65
24-hr	GEV_0-ML	1.63	0.35	-0.091	***-303.66***	3.45	5.98	1.73
	GEV_0-DEMC	1.77	0.46	0.078	-297.29	3.29	6.18	1.88
	GEV_t-I	1.67 + 0.005*t*	0.44	0.058	**-302.87**	3.36	5.14	1.53
	GEV_t-II	1.52 + 0.011*t*	exp(1.52 + 0.0066*t*)	-0.041	-281.85	3.39	4.7	1.39

Table S21. Performance of stationary and nonstationary models for London Int'l Airport

Time Slice	Model	Location parameter	Scale parameter	Shape parameter	AIC_c	LB (100yr)	UB (100yr)	UB/LB
15-min	GEV_0-ML	46.64	15.43	-0.11	***-453.96***	123.27	225.91	1.83
	GEV_0-DEMC	52.10	19.48	0.06	-452.25	115.91	219.76	1.89
	GEV_t-I	59.55-0.23*t*	16.81	0.17	**-475.09**	120.97	253.18	2.09
	GEV_t-II	49.12+0.067*t*	exp(2.24+0.016*t*)	0.12	-435.12	125.56	177.29	1.41
30-min	GEV_0-ML	30.96	8.59	-0.046	-516.96	82.54	187.38	2.27
	GEV_0-DEMC	34.01	10.70	0.17	***-521.30***	73.66	187.21	2.54
	GEV_t-I	36.74-0.080*t*	10.89	0.16	**-525.86**	78.26	171.1	2.19
	GEV_t-II	31.12+0.078*t*	exp(1.83+0.016*t*)	0.018	-438.09	74.71	97.69	1.31
1-hr	GEV_0-ML	17.34	5.56	-0.050	-518.21	49.49	104.65	2.11
	GEV_0-DEMC	19.42	7.04	0.15	***-525.00***	46.67	103.41	2.21
	GEV_t-I	20.70-0.046*t*	6.86	0.14	**-516.29**	54.2	76.28	1.41
	GEV_t-II	22.42-0.025*t*	exp(1.87+0.0057*t*)	0.15	-494.12	83.11	114.89	1.38
2-hr	GEV_0-ML	10.66	3.72	-0.122	***-498.15***	28.94	52.01	1.80
	GEV_0-DEMC	11.59	4.42	0.052	-461.02	26.32	55.01	2.09
	GEV_t-I	13.75-0.04*t*	4.71	0.003	**-491.92**	28.95	42.53	1.47
	GEV_t-II	13.10-0.029*t*	exp(1.37+0.0035*t*)	-0.049	-478.48	27.21	34.62	1.27
6-hr	GEV_0-ML	4.80	1.13	-0.098	-506.14	10.63	18.67	1.76
	GEV_0-DEMC	5.21	1.34	0.076	***-511.82***	10.02	19.27	1.92
	GEV_t-I	5.82-0.02*t*	1.31	0.13	**-496.47**	11.01	16.65	1.51
	GEV_t-II	5.81-0.019*t*	exp(0.322-0.002*t*)	0.089	-494.35	10.66	15.23	1.43
12-hr	GEV_0-ML	2.89	0.66	-0.171	***-520.41***	5.85	9.05	1.55
	GEV_0-DEMC	3.10	0.82	0.006	-518.53	5.71	9.38	1.64
	GEV_t-I	3.42-0.009*t*	0.80	-0.004	**-528.75**	6.07	7.67	1.26
	GEV_t-II	3.43-0.0093*t*	exp(-0.21-0.0012*t*)	-0.03	-505.09	5.87	7.14	1.22
24-hr	GEV_0-ML	1.55	0.51	-0.28	-458.39	3.57	5.85	1.64
	GEV_0-DEMC	1.74	0.64	-0.07	***-469.91***	3.28	6.06	1.85
	GEV_t-I	1.99 – 0.008*t*	0.62	-0.05	**-463.94**	3.54	5.47	1.54
	GEV_t-II	2.07 – 0.0089*t*	exp(-0.44-0.0012*t*)	-0.09	-439.12	3.31	5.11	1.54

Table S22. Performance of stationary and nonstationary models for Trenton Airport

Time Slice	Model	Location parameter	Scale parameter	Shape parameter	AIC_c	LB (100yr)	UB (100yr)	UB/LB
15-min	GEV_0-ML	38.711	9.46	0.073	-492.50	109.41	274.56	2.51
	GEV_0-DEMC	42.15	12.00	0.264	***-494.40***	105.99	247.42	2.33
	GEV_t-I	44.25-0.082*t*	11.56	0.301	-488.20	134.54	186.66	1.39
	GEV_t-II	40.72+0.045*t*	exp(1.92+0.016*t*)	0.291	**-498.80**	129.24	185.41	1.43
30-min	GEV_0-ML	24.86	6.70	-0.065	***-500.61***	63.03	132.64	2.10
	GEV_0-DEMC	27.30	8.32	0.119	-498.56	57.82	121.78	2.11
	GEV_t-I	27.94 – 0.029*t*	8.34	0.171	**-501.76**	60.58	126.29	2.08
	GEV_t-II	26.22 + 0.036*t*	exp(1.58 + 0.0154*t*)	0.142	-500.42	66.88	98.13	1.47
1-hr	GEV_0-ML	14.94	4.09	-0.05	-467.40	39.95	95.1	2.38
	GEV_0-DEMC	16.52	5.24	0.16	***-475.82***	36.66	87.35	2.38
	GEV_t-I	16.21 + 0.015*t*	5.44	0.17	**-484.48**	38.86	80.42	2.07
	GEV_t-II	15.56 + 0.032*t*	exp(1.58 + 0.004*t*)	0.22	-479.32	53.31	69.24	1.30
2-hr	GEV_0-ML	9.17	2.59	-0.042	-511.03	24.9	57.96	2.33
	GEV_0-DEMC	10.07	3.35	0.18	***-525.68***	23.24	52.3	2.25
	GEV_t-I	9.195 + 0.025*t*	3.35	0.20	**-527.73**	30.19	41.44	1.37
	GEV_t-II	9.157 + 0.042*t*	exp(1.21 + 0.003*t*)	0.12	-479.09	26.44	42.43	1.60
6-hr	GEV_0-ML	4.77	1.10	-0.041	***-426.09***	11.05	21.35	1.93
	GEV_0-DEMC	5.15	1.41	0.132	-425.70	10.42	21.31	2.05
	GEV_t-I	4.77 + 0.012*t*	1.33	0.179	**-436.47**	11.84	18.7	1.58
	GEV_t-II	4.71 + 0.013*t*	exp(0.295 + 0.0009*t*)	0.162	-432.69	12.95	17.13	1.32
12-hr	GEV_0-ML	2.98	0.699	-0.082	-493.45	6.75	12.61	1.87
	GEV_0-DEMC	3.22	0.875	0.11	***-497.49***	6.38	11.54	1.81
	GEV_t-I	2.85 + 0.011*t*	0.842	0.14	**-498.05**	7.58	10.07	1.33
	GEV_t-II	2.85 + 0.011*t*	exp(-0.20 + 0.0023*t*)	0.12	-498.42	6.88	11.35	1.65
24-hr	GEV_0-ML	1.75	0.42	-0.25	***-489.02***	3.54	5.41	1.53
	GEV_0-DEMC	1.87	0.51	0.043	-478.26	3.35	5.65	1.69
	GEV_t-I	1.64 + 0.0075*t*	0.49	-0.014	-487.79	3.4	5.36	1.58
	GEV_t-II	1.63 + 0.0081*t*	Exp(-0.68 + 0.00063*t*)	-0.026	**-499.42**	3.64	4.73	1.30

Table S23. Performance of stationary and nonstationary models for Stratford WWTP

Time Slice	Model	Location parameter	Scale parameter	Shape parameter	AIC_c	LB (100yr)	UB (100yr)	UB/LB
15-min	GEV_0-ML	51.80	11.88	-0.1412	***-430.48***	109.78	194.73	1.77
	GEV_0-DEMC	55.50	14.68	0.047	-411.76	102.2	190.08	1.86
	GEV_t-I	57.50 – 0.051*t*	14.94	0.038	-425.73	114.09	152.58	1.34
	GEV_t-II	45.55 + 0.364*t*	exp(1.99 – 0.022*t*)	0.120	**-446.456**	114.24	199.3	1.74
30-min	GEV_0-ML	31.21	8.49	-0.047	-434.86	82.98	199.55	2.40
	GEV_0-DEMC	34.46	11.08	0.173	***-442.47***	78.81	189.95	2.41
	GEV_t-I	35.56-0.0085*t*	11.17	0.0084	-402.18	73.23	107	1.46
	GEV_t-II	36.12 – 0.07*t*	exp(2.49 – 0.0018*t*)	0.253	**-423.75**	111.47	159.54	1.43
1-hr	GEV_0-ML	16.89	4.78	0.023	***-392.87***	51.48	158.89	3.09
	GEV_0-DEMC	18.84	6.19	0.24	-386.66	48.26	112.41	2.33
	GEV_t-I	18.9 – 0.0044*t*	6.64	0.17	-387.61	53.75	82.71	1.53
	GEV_t-II	18.77 + 0.013*t*	exp(1.91+0.001*t*)	0.29	**-401.6**	69.69	108.79	1.56
2-hr	GEV_0-ML	10.28	3.21	-0.0021	***-387.57***	35.2	155.07	4.41
	GEV_0-DEMC	11.61	4.29	0.26	-379.62	31.62	110.1	3.48
	GEV_t-I	12.005-0.0057*t*	4.52	0.24	**-400.61**	32.68	90.23	2.76
	GEV_t-II	11.48+0.0047*t*	exp(1.37+0.0052*t*)	0.46	-369.25	38.4	117.1	3.05
6-hr	GEV_0-ML	4.81	1.40	0.046	***-404.38***	8.36	24.44	2.92
	GEV_0-DEMC	5.33	1.85	0.22	-397.23	13.52	35.07	2.59
	GEV_t-I	5.69-0.012*t*	1.75	0.25	**-402.09**	15.23	32.76	2.15
	GEV_t-II	5.75-0.010*t*	exp(0.73-0.00256*t*)	0.26	-397.00	18.8	27.61	1.47
12-hr	GEV_0-ML	2.85	0.694	0.088	***-375.20***	8.36	24.44	2.92
	GEV_0-DEMC	3.14	0.913	0.289	-373.23	8.0	20.78	2.60
	GEV_t-I	3.40-0.010*t*	0.863	0.345	**-380.61**	10.93	15.69	1.44
	GEV_t-II	3.42 – 0.0097*t*	exp(-0.143 + 0.0013*t*)	0.279	-371.54	7.9	17.86	2.26
24-hr	GEV_0-ML	1.53	0.353	0.077	***-383.44***	4.24	11.67	2.75
	GEV_0-DEMC	1.69	0.463	0.217	-365.50	3.98	7.27	1.83
	GEV_t-I	1.80 – 0.0049*t*	0.457	0.306	**-388.25**	4.98	8.0	1.61
	GEV_t-II	1.83 – 0.0055*t*	exp(-0.71-0.0025*t*)	0.252	-374.37	4.57	7.1	1.55

Table S24. Performance of stationary and nonstationary models for Fergas Shand Dam

Time Slice	Model	Location parameter	Scale parameter	Shape parameter	AIC_c	LB (100yr)	UB (100yr)	UB/LB
15-min	GEV_0-ML	53.55	16.13	-0.138	***-531.24***	130.69	228.7	1.75
	GEV_0-DEMC	58.35	21.53	0.029	-496.03	114.98	269.92	2.35
	GEV_t-I	49.36 + 0.314*t*	22.64	-0.107	**-467.56**	113.15	182.83	1.62
	GEV_t-II	23.51 + 0.855*t*	exp(2.91 + 0.0086*t*)	-0.152	-328.39	108.48	168.75	1.56
30-min	GEV_0-ML	33.98	10.79	-0.049	***-470.19***	93.46	178.37	1.91
	GEV_0-DEMC	37.67	13.36	0.096	-465.55	62.26	147.67	2.37
	GEV_t-I	39.72 – 0.057*t*	13.51	0.065	**-457.48**	94.52	135.23	1.43
	GEV_t-II	34.02 + 0.0833*t*	exp(2.296+0.0073*t*)	0.059	-434.18	80.93	138.88	1.72
1-hr	GEV_0-ML	19.55	6.60	-0.028	-533.33	59.41	133.08	2.24
	GEV_0-DEMC	22.06	8.42	0.156	***-537.44***	47.65	104.07	2.18
	GEV_t-I	24.00 -0.075*t*	8.18	0.154	**-516.37**	56.13	119.19	2.12
	GEV_t-II	20.49 + 0.061*t*	exp(1.66 + 0.0132*t*)	0.127	-502.04	48.69	135.28	2.78
2-hr	GEV_0-ML	11.11	4.16	-0.078	-531.68	33.97	72.24	2.14
	GEV_0-DEMC	12.62	5.17	0.121	***-544.26***	27.39	49.43	1.80
	GEV_t-I	13.76-0.04*t*	5.13	0.047	-472.25	30.4	50.32	1.66
	GEV_t-II	13.66 – 0.039*t*	exp(1.62+0.0011*t*)	0.193	**-534.16**	44.21	59.35	1.34
6-hr	GEV_0-ML	4.63	1.91	-0.146	***-541.94***	13.55	23.96	1.77
	GEV_0-DEMC	5.22	2.35	0.017	-531.42	12.07	37.07	3.07
	GEV_t-I	5.45 – 0.0041*t*	2.41	-0.041	-515.89	14.25	18.33	1.29
	GEV_t-II	5.39 – 0.0041*t*	exp(0.843+0.00014*t*)	0.021	**-544.18**	14.77	18.59	1.26

Table S25. Z-statistics* between best selected nonstationary and stationary model for 50-year return period

Duration	Toronto	Hamilton	Oshawa	Windsor	Kingston	London	Trenton	Stratford	Fergus Shand
15-min	-0.061	-0.249	0.204	-0.408	0.159	0.234	0.017	0.214	-0.275
30-min	0.045	-0.317	0.065	-0.367	0.090	-0.012	0.134	0.461	-0.184
1-hour	0.082	-0.236	0.025	0.206	-0.111	-0.493	0.113	0.331	-0.087
2-hour	0.349	-0.309	0.350	-0.078	0.107	-0.065	0.106	-0.119	0.423
6-hour	0.020	0.185	0.113	0.109	0.141	0.093	0.148	-0.030	0.027
12-hour	0.074	0.159	0.090	0.641	0.006	0.031	0.078	0.116	*
24-hour	-0.006	-0.007	0.137	0.041	0.012	-0.021	0.134	0.097	*

*The standardized Z-statistic is positive (negative) with an increasing (decreasing) trend, and statistically significant at 5% and 10% significance levels when $|Z| > \pm 1.96$ and $|Z| > \pm 1.65$ respectively.

Table S26. Z-statistics between best selected nonstationary and stationary model for 100-year return period

Duration	Toronto	Hamilton	Oshawa	Windsor	Kingston	London	Trenton	Stratford	Fergus Shand
15-min	-0.055	-0.279	0.164	-0.443	0.027	0.282	0.042	0.239	-0.344
30-min	0.051	-0.330	0.077	-0.396	0.099	-0.018	0.139	0.492	-0.205
1-hour	0.077	-0.273	0.041	0.266	-0.122	-0.532	0.105	0.283	-0.075
2-hour	0.390	-0.343	0.354	-0.096	0.104	-0.101	0.117	-0.124	0.469
6-hour	0.006	0.178	0.156	0.116	0.140	0.131	0.159	-0.025	0.027
12-hour	0.070	0.159	0.075	0.735	-0.004	0.031	0.103	0.126	*
24-hour	-0.003	-0.005	0.121	0.063	0.000	-0.008	0.127	0.095	*

Table S27. Z-statistics between best selected nonstationary and stationary model for 10-year return period

Duration	Toronto	Hamilton	Oshawa	Windsor	Kingston	London	Trenton	Stratford	Fergus Shand
15-min	-0.082	-0.030	0.345	-0.197	0.527	0.035	-0.061	0.098	0.026
30-min	0.023	-0.191	0.017	-0.191	0.033	0.011	0.092	0.323	-0.075
1-hour	0.093	-0.104	-0.037	0.001	-0.035	-0.311	0.134	0.488	-0.138
2-hour	0.185	-0.182	0.298	-0.022	0.086	0.111	0.059	-0.041	0.252
6-hour	0.089	0.177	-0.034	0.090	0.128	-0.031	0.088	-0.050	0.032
12-hour	0.086	0.152	0.155	0.333	0.038	0.067	-0.014	0.048	*
24-hour	-0.021	-0.018	0.211	-0.044	0.055	-0.063	0.147	0.092	*

Table S28. Z-statistics between best selected nonstationary and stationary model for 2-year return period

Duration	Toronto	Hamilton	Oshawa	Windsor	Kingston	London	Trenton	Stratford	Fergus Shand
15-min	-0.110	0.585	0.576	0.213	-0.037	-0.211	-0.086	-0.149	0.426
30-min	-0.019	0.177	-0.060	0.268	-0.247	0.043	-0.102	-0.023	0.195
1-hour	0.064	0.059	-0.193	-0.299	0.395	-0.045	0.128	0.439	-0.294
2-hour	-0.239	0.010	0.067	0.007	-0.119	0.586	-0.045	0.251	-0.134
6-hour	0.209	-0.035	-0.268	0.180	0.058	-0.210	0.000	-0.076	0.024
12-hour	0.000	-0.060	0.281	-0.191	0.079	0.142	-0.090	-0.165	*
24-hour	-0.149	-0.065	0.263	-0.217	0.101	-0.068	0.115	0.000	*

Table S29.1 Ratio and percentage changes between updated nonstationary versus EC-generated DSI for Toronto International Airport for different durations

Duration	2-year	5-year	10-year	25-year	50-year	100-year
15-min	0.72	0.78	0.80	0.80	0.79	0.78
	[-38.1%]	[-27.4%]	[-25.5%]	[-25.6%]	[-26.8%]	[-28.6%]
30-min	0.75	0.83	0.86	0.90	0.92	0.94
	[-33.4%]	[-20.9%]	[-15.9%]	[-11.3%]	[-8.5%]	[-6.18%]
1-hour	0.97	0.97	0.98	0.99	1.008	1.02
	[-2.46%]	[-2.98%]	[-2.2%]	[-0.63%]	[0.81%]	[**2.4%**]
2-hour	0.96	0.94	0.96	1.002	1.04	1.09
	[-4.43%]	[-6.3%]	[-4.25%]	[0.20%]	[**4.25%**]	[**8.63%**]
6-hour	0.94	0.91	0.94	1.02	1.09	1.19
	[-6.03%]	[-9.72%]	[-6.29%]	[**1.62%**]	[**8.73%**]	[***16.32****%]
12-hour	0.92	0.89	0.94	1.08	1.24	1.46
	[-8.05%]	[-11.99%]	[-5.71%]	[**7.9%**]	[***19.68%***]	[***31.5%***]
24-hour	0.93	0.88	0.91	0.98	1.07	1.18
	[-7.03%]	[-13.0%]	[-10.3%]	[-1.78%]	[**6.5%**]	[***15.2%***]

*Results within brackets indicate percentage changes between updated versus EC-generated DSI. More than 1% increase in DSI is shown in bold, whereas 10% or more is marked with bold italic letters.

Table S29.2 Ratio and percentage changes between updated stationary versus EC-generated DSI for Toronto International Airport for different durations

Duration	2-year	5-year	10-year	25-year	50-year	100-year
15-min	0.73	0.79	0.81	0.81	0.81	0.80
	[-36.3%]	[-25.3%]	[-23.1%]	[-23.0%]	[-23.9%]	[-25.6%]
30-min	0.75	0.82	0.86	0.89	0.91	0.92
	[-33.1%]	[-21.1%]	[-16.5%]	[-12.4%]	[-10.0%]	[-8.08%]
1-hour	0.97	0.96	0.97	0.98	0.99	1.004
	[-2.87%]	[-3.82%]	[-3.3%]	[-2.1%]	[-0.90%]	[0.43%]
2-hour	0.98	0.94	0.93	0.95	0.97	0.99
	[-2.39%]	[-7.1%]	[-7.1%]	[-5.3%]	[-3.21%]	[-0.59%]
6-hour	0.93	0.89	0.93	1.005	1.09	1.19
	[-7.17%]	[-11.3%]	[-7.8%]	[0.47%]	[**8.03%**]	[***16.07****%]
12-hour	0.92	0.89	0.93	1.06	1.2	1.39
	[-8.05%]	[-13.01%]	[-7.4%]	[**5.3%**]	[***16.68%***]	[***28.1%***]
24-hour	0.94	0.89	0.91	0.98	1.07	1.18
	[-6.45%]	[-12.1%]	[-9.9%]	[-1.53%]	[**6.67%**]	[***15.3%***]

*More than 10% increase is marked in bold italics.

Table S30.1 Ratio and percentage changes between updated nonstationary versus EC-generated DSI for Hamilton Airport for different durations

Duration	2-year	5-year	10-year	25-year	50-year	100-year
15-min	0.98	0.96	0.95	0.95	0.95	0.95
	[-1.18%]	[-3.96%]	[-4.85%]	[-5.4%]	[-5.45%]	[-5.4%]
30-min	0.72	0.71	0.71	0.73	0.75	0.77
	[-38.3%]	[-40.8%]	[-39.8%]	[-36.5%]	[-33.3%]	[-29.6%]
1-hour	0.95	0.89	0.88	0.87	0.87	0.88
	[-4.80%]	[-11.48%]	[-13.5%]	[-14.4%]	[-14.3%]	[-13.7%]
2-hour	0.95	0.87	0.83	0.81	0.81	0.80
	[-5.15%]	[-15.78%]	[-19.7%]	[-22.6%]	[-23.7%]	[-24.2%]
6-hour	0.88	0.86	0.89	0.98	1.08	1.21
	[-12.6%]	[-16.84%]	[-12.2%]	[-1.89%]	[**7.7%**]	[***17.7%***]
12-hour	0.91	0.88	0.89	0.95	1.003	1.07
	[-9.19%]	[-13.51%]	[-11.4%]	[-5.51%]	[0.38%]	[**7.1%**]
24-hour	0.76	0.79	0.83	0.90	0.96	1.02
	[-31.3%]	[-25.76%]	[-19.8%]	[-11.1%]	[-4.2%]	[**2.57%**]

Table S30.2 Ratio and percentage changes between updated stationary versus EC-generated DSI for Hamilton Airport for different durations

Duration	2-year	5-year	10-year	25-year	50-year	100-year
15-min	0.96	0.94	0.96	0.99	1.02	1.07
	[-4.4%]	[-5.94%]	[-4.38%]	[-0.68%]	[**2.84%**]	[**6.7%**]
30-min	0.71	0.71	0.74	0.78	0.83	0.89
	[-39.6%]	[-39.9%]	[-35.8%]	[-27.6%]	[-20.4%]	[-12.6%]
1-hour	0.95	0.89	0.89	0.91	0.93	0.95
	[-5.33%]	[-11.13%]	[-11.6%]	[-10.1%]	[-7.9%]	[-5.1%]
2-hour	0.95	0.87	0.86	0.86	0.87	0.88
	[-5.2%]	[-14.43%]	[-16.5%]	[-16.4%]	[-15.1%]	[-12.9%]
6-hour	0.88	0.84	0.86	0.92	0.99	1.09
	[-12.4%]	[-18.52%]	[-16.0%]	[-8.13%]	[-0.2%]	[**8.4%**]
12-hour	0.91	0.87	0.87	0.91	0.95	1.005
	[-8.87%]	[-14.54%]	[-14.0%]	[-9.59%]	[-4.89%]	[0.57%]
24-hour	0.76	0.80	0.84	0.90	0.96	1.03
	[-30.5%]	[-24.67%]	[-19.4%]	[-10.8%]	[-3.96%]	[**2.76%**]

Table S31.1 Ratio and percentage changes between updated nonstationary versus EC-generated DSI for Oshawa WPCP for different durations

Duration	2-year	5-year	10-year	25-year	50-year	100-year
15-min	1.10	1.11	1.10	1.07	1.05	1.02
	[**9.18%**]	[***10.2*%**]	[**9.21%**]	[**6.95%**]	[**4.8%**]	[**2.35%**]
30-min	1.06	1.05	1.02	0.98	0.95	0.92
	[**5.76%**]	[**4.73%**]	[**2.5%**]	[-1.28%]	[-4.5%]	[-8.12%]
1-hour	1.01	1.05	1.08	1.09	1.10	1.11
	[**1.89%**]	[**5.5%**]	[**7.06%**]	[**8.54%**]	[**9.41%**]	[***10.14*%**]
2-hour	1.02	1.07	1.13	1.21	1.29	1.38
	[**2.11%**]	[**6.71%**]	[***11.2*%**]	[***17.61*%]	[***22.6*%]	[***27.51*%]
6-hour	0.99	0.99	1.02	1.06	1.10	1.15
	[-0.91%]	[-0.27%]	[**1.85%**]	[**5.88%**]	[**9.3%**]	[***12.9*%**]
12-hour	0.98	0.89	0.91	0.97	1.05	1.15
	[-1.89%]	[-11.6%]	[-9.94%]	[-2.66%]	[**5.00%**]	[***13.5*%**]
24-hour	0.99	0.95	0.97	1.005	1.04	1.09
	[-0.54%]	[-4.31%]	[-3.2%]	[0.51%]	[**4.2%**]	[**8.52%**]

Table S31.2 Ratio and percentage changes between updated stationary versus EC-generated DSI for Oshawa WPCP for different durations

Duration	2-year	5-year	10-year	25-year	50-year	100-year
15-min	1.05	1.04	1.03	1.00	0.98	0.96
	[**5.04%**]	[**4.25%**]	[**2.84%**]	[0.50%]	[-1.50%]	[-3.69%]
30-min	1.06	1.05	1.02	0.98	0.93	0.90
	[**6.31%**]	[**4.94%**]	[**2.18%**]	[-2.44%]	[-6.5%]	[-10.8%]
1-hour	1.04	1.07	1.08	1.09	1.09	1.09
	[**4.03%**]	[**6.8%**]	[**7.76%**]	[**8.42%**]	[**8.69%**]	[**8.83%**]
2-hour	1.01	1.03	1.06	1.10	1.14	1.19
	[**1.5%**]	[**3.2%**]	[**5.65%**]	[**9.51%**]	[***12.6*%**]	[***15.95*%**]
6-hour	1.01	1.01	1.02	1.04	1.07	1.09
	[**1.26%**]	[**1.5%**]	[**2.42%**]	[**4.61%**]	[**6.4%**]	[**8.52%**]
12-hour	0.97	0.87	0.88	0.94	1.01	1.11
	[-3.5%]	[-14.25%]	[-13.1%]	[-6.07%]	[**1.53%**]	[**9.99%**]
24-hour	0.98	0.93	0.94	0.96	1.00	1.04
	[-2.18%]	[-7.25%]	[-6.7%]	[-3.78%]	[0%]	[**3.98%**]

Table S32.1 Ratio and percentage changes between updated nonstationary versus EC-generated DSI for Windsor Airport for different durations

Duration	2-year	5-year	10-year	25-year	50-year	100-year
15-min	0.98	0.97	0.97	0.97	0.96	0.96
	[-1.71%]	[-2.4%]	[-2.85%]	[-3.36%]	[-3.7%]	[-4.09%]
30-min	1.01	1.02	1.01	1.003	0.99	0.98
	[**1.81%**]	[**2.18%**]	[**1.59%**]	[0.35%]	[-0.81%]	[-2.11%]
1-hour	0.98	0.99	1.009	1.05	1.08	1.11
	[-1.48%]	[-0.96%]	[0.96%]	[**4.39%**]	[**7.4%**]	[***10.54*%**]
2-hour	1.06	1.06	1.04	1.005	0.97	0.94
	[**6.23%**]	[**5.92%**]	[**4.02%**]	[0.55%]	[-2.5%]	[-5.91%]
6-hour	1.04	1.06	1.07	1.10	1.12	1.15
	[**3.97%**]	[**5.58%**]	[**7.05%**]	[**9.34%**]	[***11.11*%**]	[***13.02*%**]
12-hour	0.99	1.03	1.08	1.17	1.26	1.36
	[-0.78%]	[**2.71%**]	[**7.53%**]	[***14.9*%**]	[***20.82*%**]	[***26.81*%**]
24-hour	0.99	1.003	1.01	1.03	1.05	1.07
	[-0.45%]	[0.35%]	[**1.82%**]	[**3.6%**]	[**5.07%**]	[**6.64%**]

Table S32.2 Ratio and percentage changes between updated stationary versus EC-generated DSI for Windsor Airport for different durations

Duration	2-year	5-year	10-year	25-year	50-year	100-year
15-min	0.96	0.97	1.007	1.04	1.07	1.11
	[-3.11%]	[-2.12%]	[0.06%]	[**3.85%**]	[**7.13%**]	[***10.61*%**]
30-min	0.99	1.02	1.05	1.08	1.11	1.14
	[-0.56%]	[**2.65%**]	[**4.97%**]	[**7.98%**]	[***10.24*%**]	[***12.49*%**]
1-hour	1.009	1.006	1.009	1.02	1.02	1.03
	[0.90%]	[0.62%]	[0.94%]	[**1.72%**]	[**2.44%**]	[**3.25%**]
2-hour	1.06	1.06	1.04	1.01	0.99	0.96
	[**6.18%**]	[**5.88%**]	[**4.32%**]	[**1.56%**]	[-0.94%]	[-3.64%]
6-hour	1.02	1.05	1.06	1.08	1.09	1.11
	[**2.73%**]	[**4.56%**]	[**5.76%**]	[**7.5%**]	[**8.71%**]	[***10.02*%**]
12-hour	1.005	1.01	1.03	1.05	1.08	1.10
	[0.52%]	[**1.18%**]	[**2.69%**]	[**5.07%**]	[**7.33%**]	[**9.5%**]
24-hour	1.009	1.02	1.02	1.03	1.04	1.05
	[0.89%]	[**1.74%**]	[**2.42%**]	[**3.35%**]	[**4.18%**]	[**5.06%**]

Table S33.1 Ratio and percentage changes between updated nonstationary versus EC-generated DSI for Kingston P. Station for different durations

Duration	2-year	5-year	10-year	25-year	50-year	100-year
15-min	0.98	1.13	1.12	1.07	1.01	0.96
	[-2.01%]	[***11.5%***]	[***11.02%***]	[**6.55%**]	[**1.71%**]	[-3.9%]
30-min	0.96	0.97	0.97	0.96	0.95	0.94
	[-3.31%]	[-3.03%]	[-3.42%]	[-4.22%]	[-5.00%]	[-5.86%]
1-hour	1.002	0.96	0.93	0.89	0.86	0.83
	[0.24%]	[-3.72%]	[-7.12%]	[-11.9%]	[-15.8%]	[-19.95%]
2-hour	0.96	0.95	0.95	0.97	0.98	0.99
	[-4.03%]	[-5.41%]	[-4.95%]	[-3.4%]	[-1.8%]	[-0.10%]
6-hour	0.99	0.98	1.0	1.03	1.06	1.11
	[-0.69%]	[-1.58%]	[0%]	[**3.34%**]	[**6.3%**]	[**9.65%**]
12-hour	0.98	0.98	0.99	1.03	1.07	1.12
	[-1.17%]	[-2.23%]	[-0.37%]	[**3.38%**]	[**7.1%**]	[***11.02%***]
24-hour	0.99	0.98	0.99	0.99	1.01	1.02
	[-0.51%]	[-1.20%]	[-1.05%]	[-0.29%]	[**1.07%**]	[**1.94%**]

Table S33.2 Ratio and percentage changes between updated stationary versus EC-generated DSI for Kingston P. Station for different durations

Duration	2-year	5-year	10-year	25-year	50-year	100-year
15-min	0.98	0.98	0.98	0.97	0.96	0.95
	[-1.5%]	[-1.6%]	[-2.11%]	[-3.13%]	[-4.04%]	[-5.01%]
30-min	0.98	0.97	0.96	0.94	0.93	0.91
	[-1.1%]	[-2.6%]	[-4.03%]	[-6.07%]	[-7.74%]	[-9.44%]
1-hour	0.98	0.96	0.93	0.91	0.88	0.86
	[-1.6%]	[-4.19%]	[-6.67%]	[-10.2%]	[-13.1%]	[-16.11%]
2-hour	0.97	0.94	0.94	0.95	0.95	0.96
	[-3.4%]	[-5.81%]	[-6.13%]	[-5.6%]	[-4.87%]	[-3.88%]
6-hour	0.98	0.97	0.98	1.004	1.03	1.06
	[-1.04%]	[-2.79%]	[-1.82%]	[0.47%]	[**2.89%**]	[**5.62%**]
12-hour	0.98	0.97	0.99	1.03	1.07	1.12
	[-1.77%]	[-2.69%]	[-0.95%]	[**3.09%**]	[**6.94%**]	[***11.12*%**]
24-hour	0.99	0.98	0.98	0.99	1.01	1.02
	[-1.03%]	[-2.02%]	[-1.76%]	[-0.59%]	[0.8%]	[**1.94%**]

Table S34.1 Ratio and percentage changes between updated nonstationary versus EC-generated DSI for London International Airport for different durations

Duration	2-year	5-year	10-year	25-year	50-year	100-year
15-min	0.91	0.92	0.95	1.01	1.06	1.12
	[-10.01%]	[-8.19%]	[-4.54%]	[**1.32%**]	[**6.16%**]	[***11.17%***]
30-min	0.93	0.93	0.95	1.004	1.05	1.10
	[-7.9%]	[-7.4%]	[-4.62%]	[0.38%]	[**4.72%**]	[**9.30%**]
1-hour	0.89	0.88	0.88	0.91	0.95	0.98
	[-12.6%]	[-14.83%]	[-13.1%]	[-9.26%]	[-5.58%]	[-1.56%]
2-hour	0.95	0.94	0.94	0.94	0.93	0.93
	[-4.97%]	[-6.07%]	[-6.48%]	[-6.8%]	[-6.94%]	[-7.02%]
6-hour	0.92	0.92	0.93	0.95	0.98	1.02
	[-8.14%]	[-8.87%]	[-7.46%]	[-4.25%]	[-1.27%]	[**2.09%**]
12-hour	0.958	0.962	0.963	0.963	0.963	0.962
	[-4.39%]	[-3.93%]	[-3.85%]	[-3.87%]	[-3.85%]	[-3.98%]
24-hour	0.924	0.953	0.956	0.957	0.951	0.945
	[-8.16%]	[-4.94%]	[-4.59%]	[-4.49%]	[-5.10%]	[-5.85%]

Table S34.2 Ratio and percentage changes between updated stationary versus EC-generated DSI for London International Airport for different durations

Duration	2-year	5-year	10-year	25-year	50-year	100-year
15-min	0.91	0.93	0.95	0.97	0.993	1.012
	[-8.95%]	[-6.91%]	[-5.13%]	[-2.66%]	[-0.74%]	[**1.21%**]
30-min	0.92	0.93	0.95	1.005	1.05	1.112
	[-8.25%]	[-7.83%]	[-4.87%]	[0.50%]	[**5.17%**]	[***10.09%***]
1-hour	0.90	0.89	0.91	0.946	0.984	1.029
	[-11.06%]	[-12.44%]	[-10.2%]	[-5.71%]	[-1.60%]	[**2.81%**]
2-hour	0.91	0.92	0.92	0.938	0.949	0.961
	[-8.84%]	[-8.81%]	[-8.03%]	[-6.6%]	[-5.36%]	[-4.04%]
6-hour	0.94	0.93	0.93	0.950	0.964	0.982
	[-6.63%]	[-7.54%]	[-6.96%]	[-5.26%]	[-3.64%]	[-1.79%]
12-hour	0.95	0.96	0.96	0.958	0.958	0.956
	[-5.0%]	[-4.41%]	[-4.49%]	[-4.43%]	[-4.35%]	[-4.59%]
24-hour	0.93	0.96	0.96	0.965	0.956	0.947
	[-7.61%]	[-4.15%]	[-3.57%]	[-3.62%]	[-4.56%]	[-5.61%]

Table S35.1 Ratio and percentage changes between updated nonstationary versus EC-generated DSI for Trenton Airport for different durations

Duration	2-year	5-year	10-year	25-year	50-year	100-year
15-min	0.98	0.99	1.049	1.156	1.265	1.400
	[-1.48%]	[-0.27%]	[**4.72%**]	[***13.55%***]	[***20.98***%]	[***28.57***%]
30-min	0.98	1.01	1.050	1.118	1.179	1.248
	[-1.83%]	[**1.11**%]	[**4.84**%]	[***10.6%***]	[***15.18***%]	[***19.88***%]
1-hour	0.98	0.955	0.970	1.012	1.055	1.107
	[-1.71%]	[-4.62%]	[-3.04%]	[**1.18%**]	[**5.25%**]	[**9.70%**]
2-hour	0.95	0.948	0.976	1.035	1.093	1.163
	[-4.42%]	[-5.42%]	[-2.46%]	[**3.41%**]	[**8.55%**]	[***14.01%***]
6-hour	0.99	0.994	1.020	1.074	1.127	1.188
	[-0.88%]	[-0.53%]	[**2.04%**]	[**6.89%**]	[***11.30%***]	[***15.86***%]
12-hour	0.99	1.015	1.042	1.087	1.131	1.181
	[-0.56%]	[**1.51%**]	[**4.04%**]	[**8.03%**]	[***11.62%***]	[***15.29***%]
24-hour	1.03	1.047	1.048	1.051	1.049	1.045
	[**2.87%**]	[**4.51%**]	[**4.62%**]	[**4.87%**]	[**4.7%**]	[**4.35%**]

Table S35.2 Ratio and percentage changes between updated stationary versus EC-generated DSI for Trenton Airport for different durations

Duration	2-year	5-year	10-year	25-year	50-year	100-year
15-min	0.99	1.009	1.060	1.160	1.259	1.379
	[-0.85%]	[0.93%]	[**5.69%**]	[***13.82%***]	[***20.58%***]	[***27.49***%]
30-min	0.98	1.006	1.034	1.083	1.127	1.178
	[-1.19%]	[0.61%]	[**3.32%**]	[**7.69%**]	[***11.31%***]	[***15.08%***]
1-hour	0.97	0.936	0.944	0.977	1.013	1.057
	[-2.81%]	[-6.84%]	[-5.88%]	[-2.34%]	[**1.31%**]	[**5.41%**]
2-hour	0.96	0.945	0.966	1.015	1.063	1.120
	[-4.05%]	[-5.75%]	[-3.47%]	[**1.47%**]	[**5.89%**]	[***10.71%***]
6-hour	0.99	0.990	1.009	1.048	1.086	1.131
	[-0.88%]	[-0.94%]	[0.91%]	[**4.61%**]	[**7.96%**]	[***11.56%***]
12-hour	1.0	1.022	1.044	1.080	1.11	1.152
	[0%]	[**2.15%**]	[**4.22%**]	[**7.47%**]	[***10.2%***]	[***13.18%***]
24-hour	1.02	1.035	1.034	1.030	1.027	1.020
	[**2.40%**]	[**3.42%**]	[**3.34%**]	[**2.92%**]	[**2.67%**]	[**1.98%**]

Table S36.1 Ratio and percentage changes between updated nonstationary versus EC-generated DSI for Stratford WWTP for different durations

Duration	2-year	5-year	10-year	25-year	50-year	100-year
15-min	0.985	0.994	1.014	1.050	1.083	1.121
	[-1.47%]	[-0.53%]	[**1.41%**]	[**4.79%**]	[**7.69%**]	[***10.81%***]
30-min	0.966	1.008	1.070	1.181	1.286	1.410
	[-3.47%]	[0.78%]	[**6.55%**]	[***15.32%***]	[***22.24%***]	[***29.10%***]
1-hour	0.934	0.971	1.039	1.169	1.294	1.447
	[-7.02%]	[-3.0%]	[**3.84%**]	[***14.46%***]	[***22.77%***]	[***30.89%***]
2-hour	0.929	0.891	0.916	0.981	1.048	1.131
	[-7.61%]	[-12.22%]	[-9.18%]	[-1.97%]	[**4.59%**]	[***11.58%***]
6-hour	0.887	0.819	0.832	0.883	0.942	1.016
	[-12.68%]	[-22.04%]	[-20.2%]	[-13.2%]	[-6.14%]	[**1.64%**]
12-hour	0.881	0.822	0.848	0.930	1.027	1.151
	[-13.41%]	[-21.71%]	[-17.9%]	[-7.49%]	[**2.64%**]	[***13.16%***]
24-hour	0.840	0.799	0.820	0.889	0.964	1.066
	[-19.02%]	[-25.20%]	[-21.9%]	[-12.5%]	[-3.72%]	[**6.05%**]

Table S36.2 Ratio and percentage changes between updated stationary versus EC-generated DSI for Stratford WWTP for different durations

Duration	2-year	5-year	10-year	25-year	50-year	100-year
15-min	0.990	0.994	1.002	1.015	1.026	1.039
	[-0.958%]	[-0.55%]	[0.17%]	[**1.45%**]	[**2.55%**]	[**3.73%**]
30-min	0.968	0.977	1.008	1.066	1.121	1.184
	[-3.26%]	[-2.29%]	[0.83%]	[**6.19%**]	[***10.76%***]	[***15.52%***]
1-hour	0.906	0.908	0.952	1.044	1.136	1.249
	[-10.32%]	[-10.14%]	[-5.04%]	[**4.20%**]	[***11.98%***]	[***19.94***%]
2-hour	0.912	0.883	0.926	1.029	1.136	1.27
	[-9.63%]	[-13.24%]	[-7.98%]	[**2.79%**]	[***12.0%***]	[***21.37***%]
6-hour	0.891	0.826	0.840	0.894	0.954	1.031
	[-12.13%]	[-21.05%]	[-19.0%]	[-11.9%]	[-4.78%]	[**2.99%**]
12-hour	0.889	0.825	0.841	0.906	0.983	1.082
	[-12.43%]	[-21.20%]	[-18.9%]	[-10.3%]	[-1.74%]	[**7.54%**]
24-hour	0.840	0.789	0.807	0.865	0.930	1.017
	[-19.02%]	[-26.69%]	[-23.9%]	[-15.6%]	[-7.52%]	[**1.67%**]

Table S37.1 Ratio and percentage changes between updated nonstationary versus EC-generated DSI for Fergus Shand dam for different durations

Duration	2-year	5-year	10-year	25-year	50-year	100-year
15-min	1.08	1.044	1.016	0.979	0.951	0.924
	[**7.12%**]	[**4.21%**]	[**1.61%**]	[-2.1%]	[-5.08%]	[-8.18%]
30-min	1.03	0.975	0.962	0.960	0.965	0.974
	[**3.33%**]	[-2.55%]	[-3.93%]	[-4.14%]	[-3.58%]	[-2.64%]
1-hour	0.961	0.900	0.901	0.927	0.958	0.996
	[-4.03%]	[-11.09%]	[-10.9%]	[-7.9%]	[-4.42%]	[-0.41%]
2-hour	0.932	0.936	0.971	1.038	1.101	1.174
	[-7.31%]	[-6.83%]	[-3.01%]	[**3.64%**]	[**9.15%**]	[***14.85%***]
6-hour	0.949	0.961	0.969	0.979	0.986	0.994
	[-5.38%]	[-4.07%]	[-3.2%]	[-2.15%]	[-1.42%]	[-0.60%]

Table S37.2 Ratio and percentage changes between updated stationary versus EC-generated DSI for Fergus Shand dam for different durations

Duration	2-year	5-year	10-year	25-year	50-year	100-year
15-min	1.043	1.017	1.012	1.013	1.016	1.022
	[**4.15%**]	[**1.75%**]	[**1.24%**]	[**1.26%**]	[**1.61%**]	[**2.13%**]
30-min	1.023	0.973	0.972	0.988	1.009	1.036
	[**2.24%**]	[-2.72%]	[-2.88%]	[-1.19%]	[0.94%]	[**3.49%**]
1-hour	0.985	0.925	0.927	0.955	0.987	1.028
	[-1.46%]	[-8.12%]	[-7.86%]	[-4.74%]	[-1.25%]	[**2.76%**]
2-hour	0.943	0.919	0.929	0.957	0.986	1.02
	[-5.97%]	[-8.75%]	[-7.61%]	[-4.44%]	[-1.40%]	[**1.97%**]
6-hour	0.947	0.957	0.965	0.974	0.981	0.987
	[-5.55%]	[-4.43%]	[-3.58%]	[-2.63%]	[-1.97%]	[-1.27%]

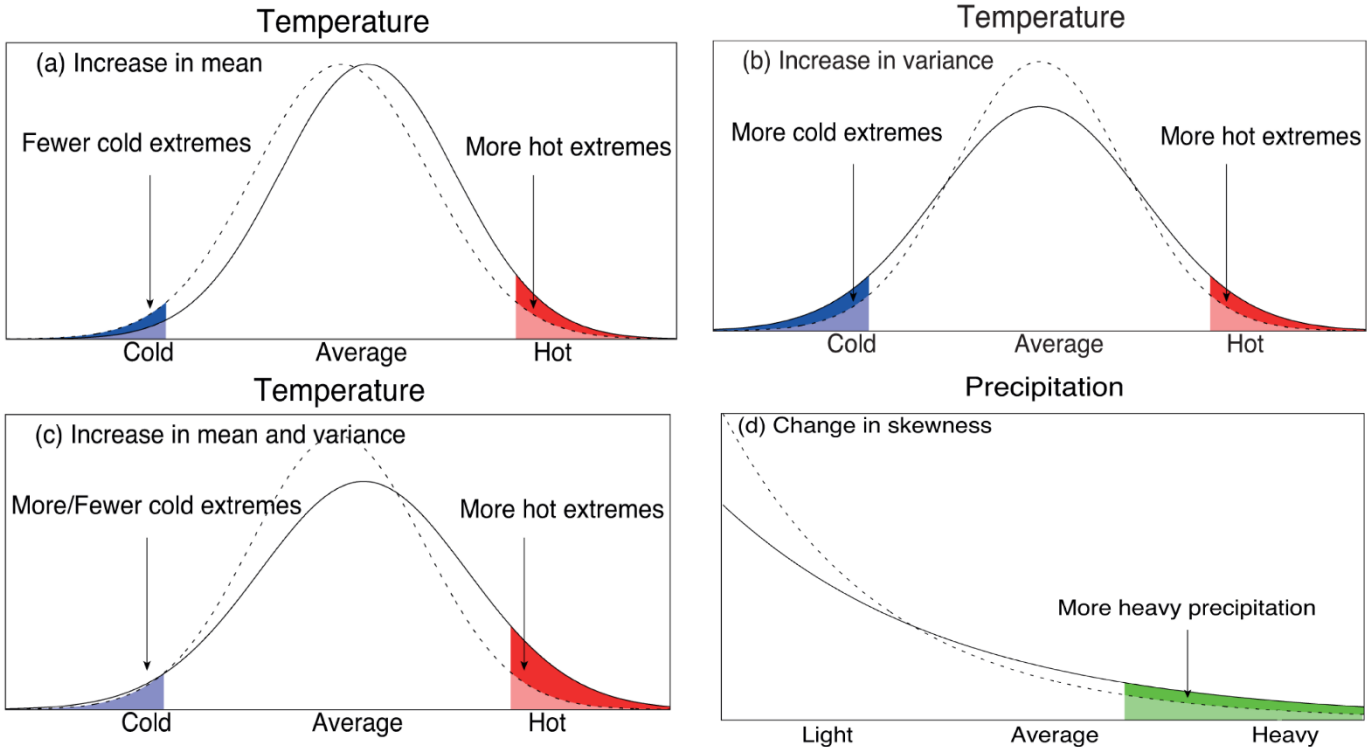

Figure S1. IPCC AR5 conceptual representation of changes in probability density functions of daily temperature (**a** – **c**) and precipitation. The previous and the new distributions are marked by the solid and the dashed lines respectively. The frequency (probability of occurrence) of extremes is denoted by the shaded areas (Source: IPCC AR5 Working Group I report, Figure 1.8, page no. 134).

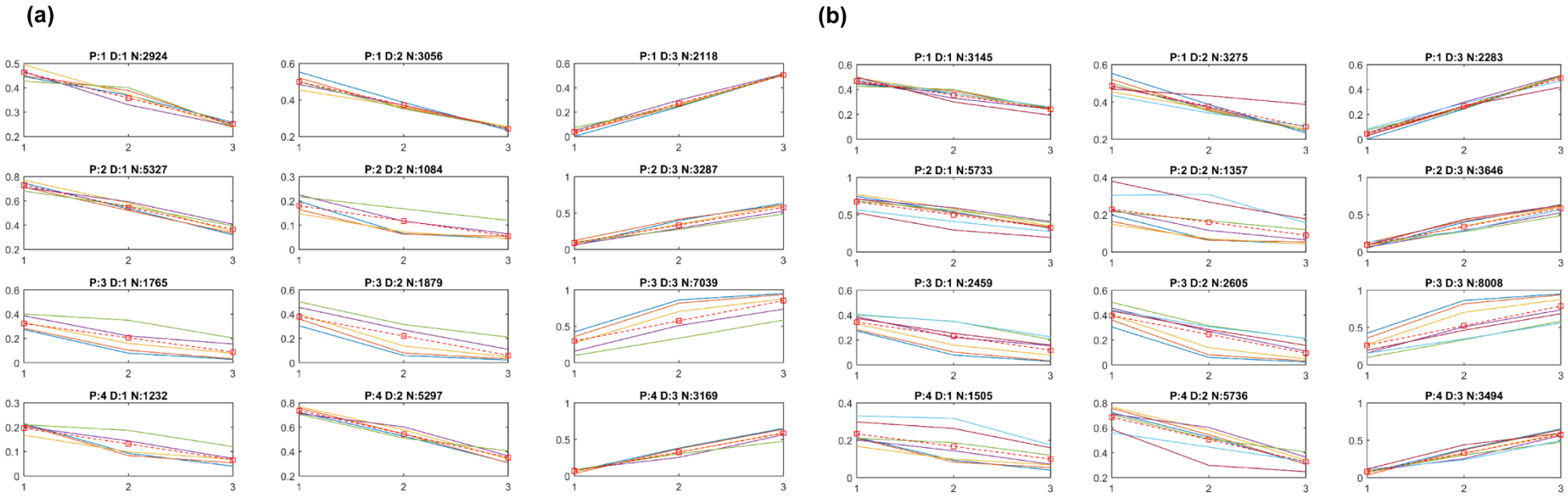

Figure S2. Variation of probabilities with volume class, v_c for Toronto International Airport at (***a***) daily to hourly-, and (***b***) daily to minute- time step disaggregation. X-axes show, v_c: 1 – small, 2 – medium, and 3 – large; Y-axes show, probabilities. *P* – denotes position type, 1: Isolated, 2: Starting, 3: Enclosed, and 4: Ending, *D* denotes division type (1: 0/1, 2: 1/0, 3: x/x), and N denotes the total number of periods for associated position and division type. The solid lines marked with different colors indicate different cascade steps. The dashed line with squares represents the mean of all cascade levels.

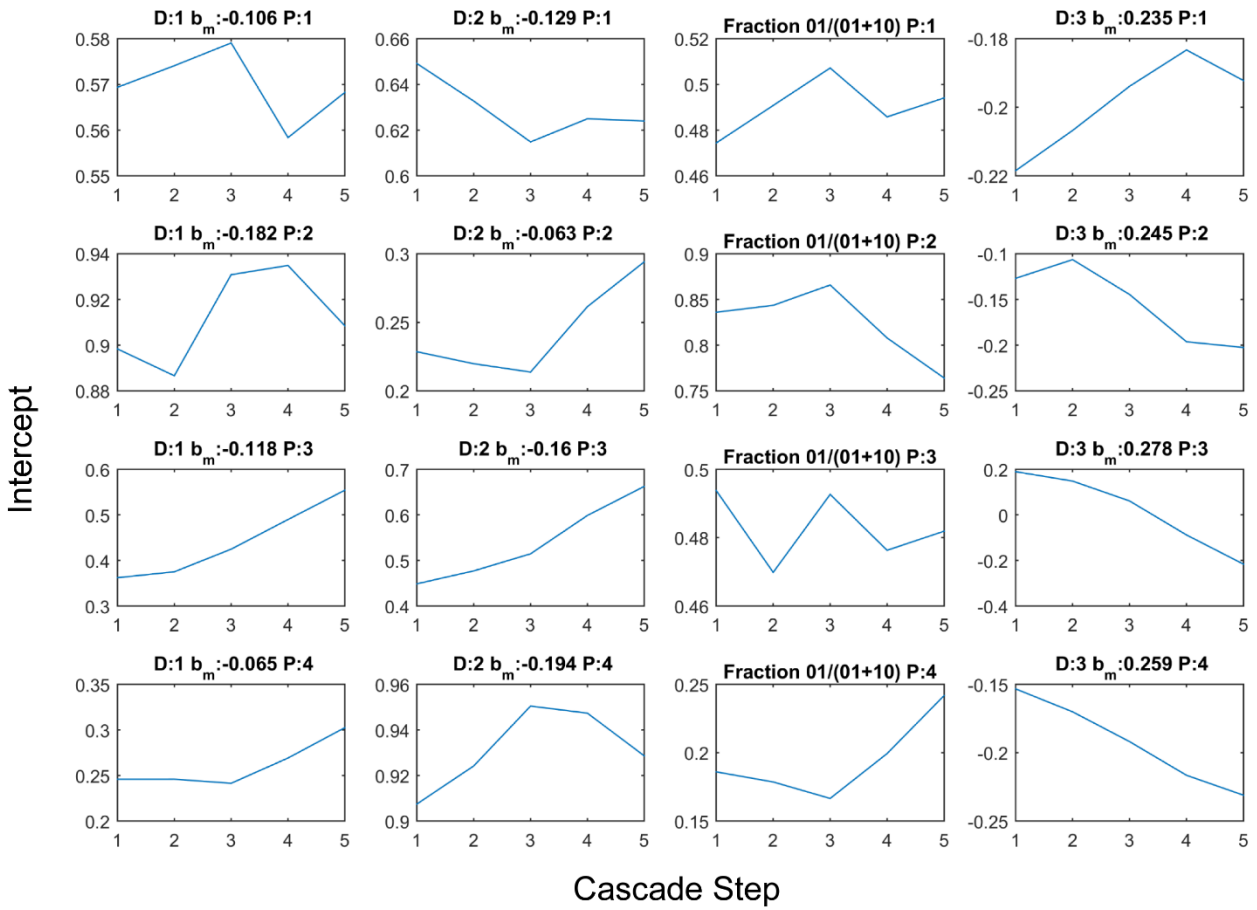

Figure S3. Variations of intercept, a_p with cascade steps for daily to hourly- time step disaggregation at Toronto International Airport. *P*-denotes position types, 1: Isolated, 2: Starting, 3: Enclosed and 4: Ending. *D* denotes division type (1: 0/1, 2: 1/0, 3: x/x), and b_m indicates the mean slope for corresponding position and division type, estimated from the fitted mean lines as in Figure S3. The third column indicates the fraction of 0/1-divisions of all "non-x/x-divisions" summed over volume classes.

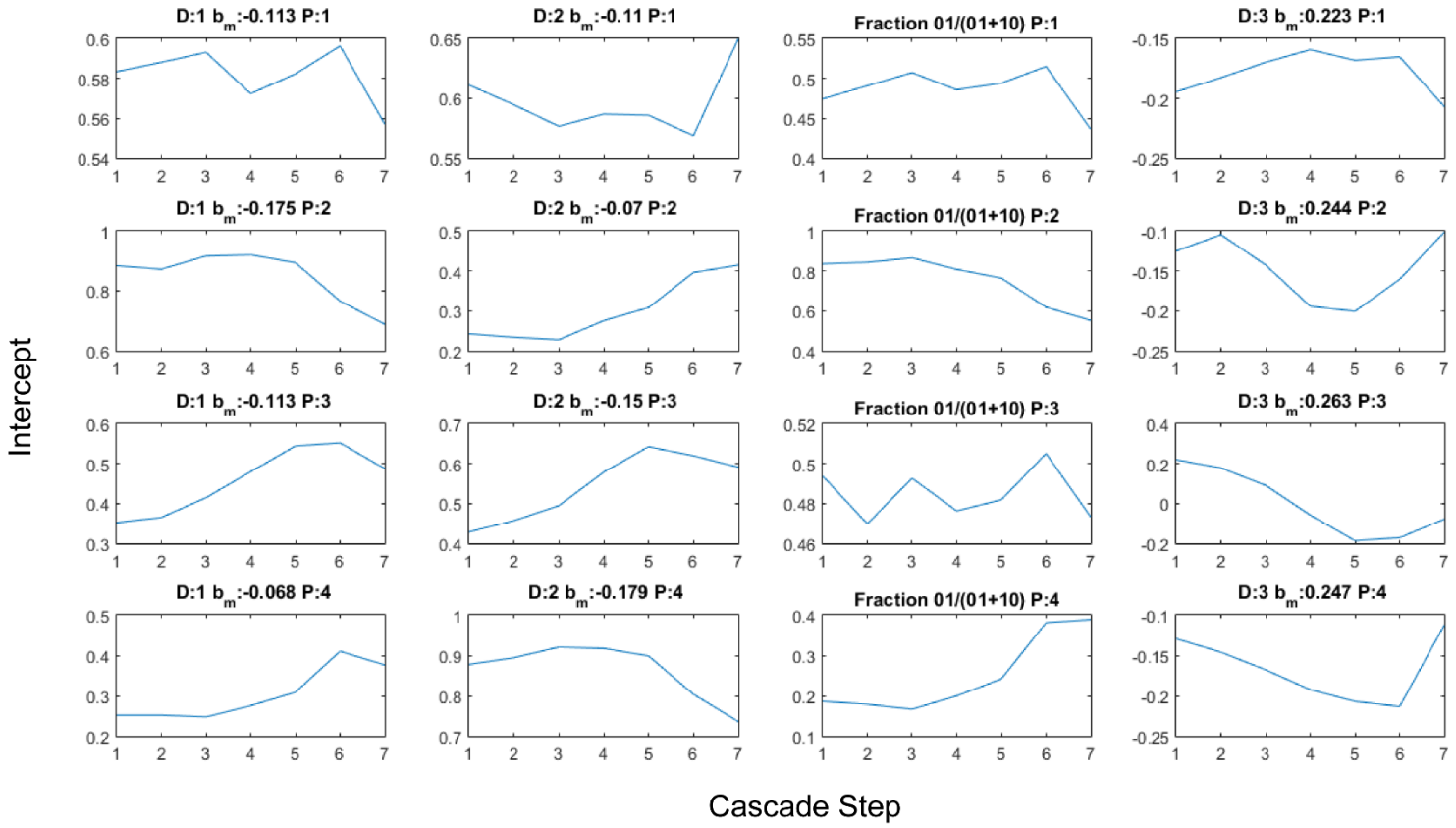

Figure S4. Same as in Figure S4 but for daily to minute- time step disaggregation.

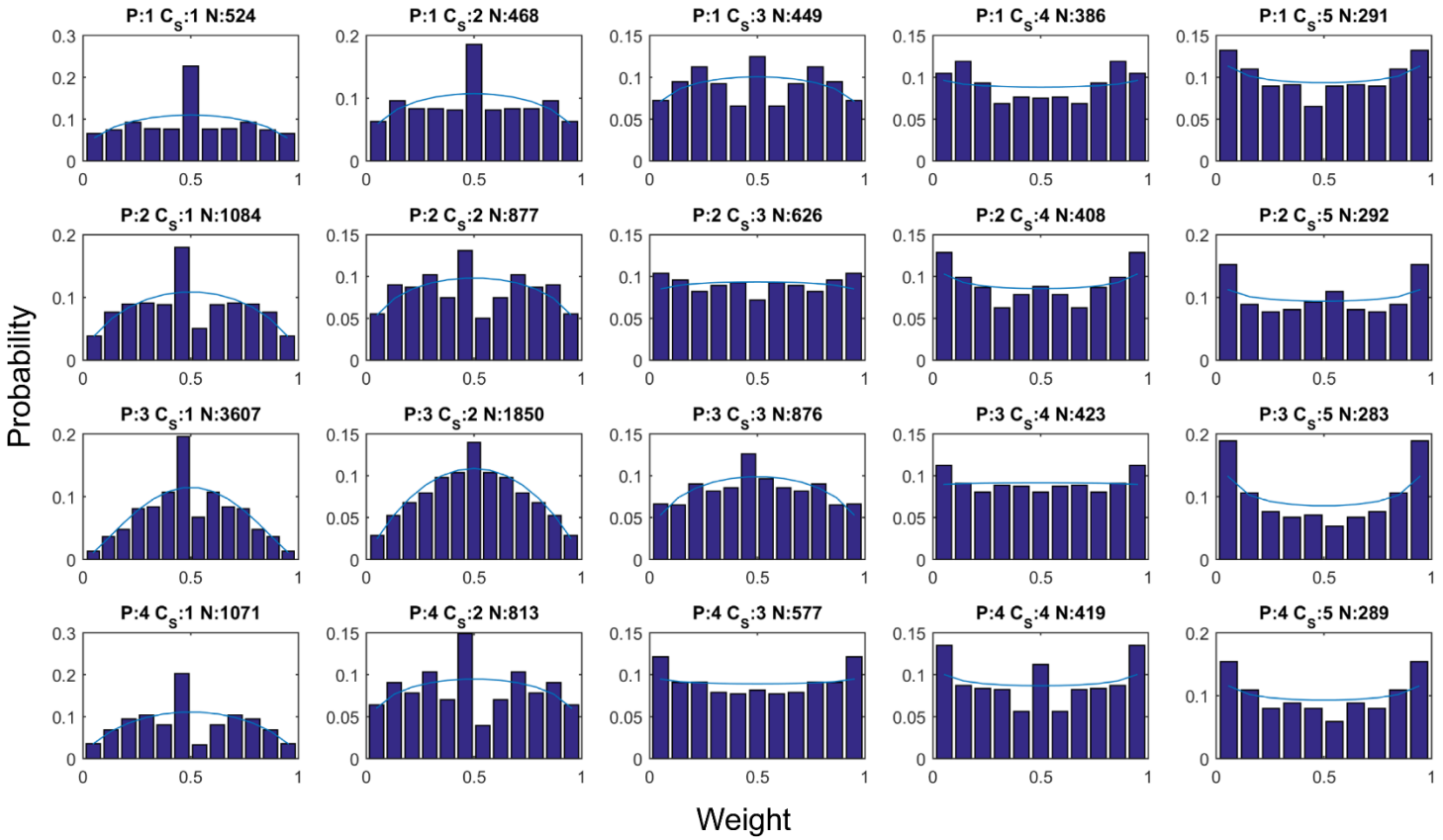

Figure S5. Variations of empirical *x/x*-distributions with cascade steps (bars) and fitted beta distributions (lines) for daily to hourly- time step disaggregation at Toronto International Airport. *P*-denotes position types, 1: Isolated, 2: Starting, 3: Enclosed and 4: Ending; C_s denotes cascade steps, for example, step 1 shows cascading from 32 to 16 minute, step 2 indicates from 16 to minute and so on. *N* indicates the total number of *x/x*- divisions for this position type and cascade level.

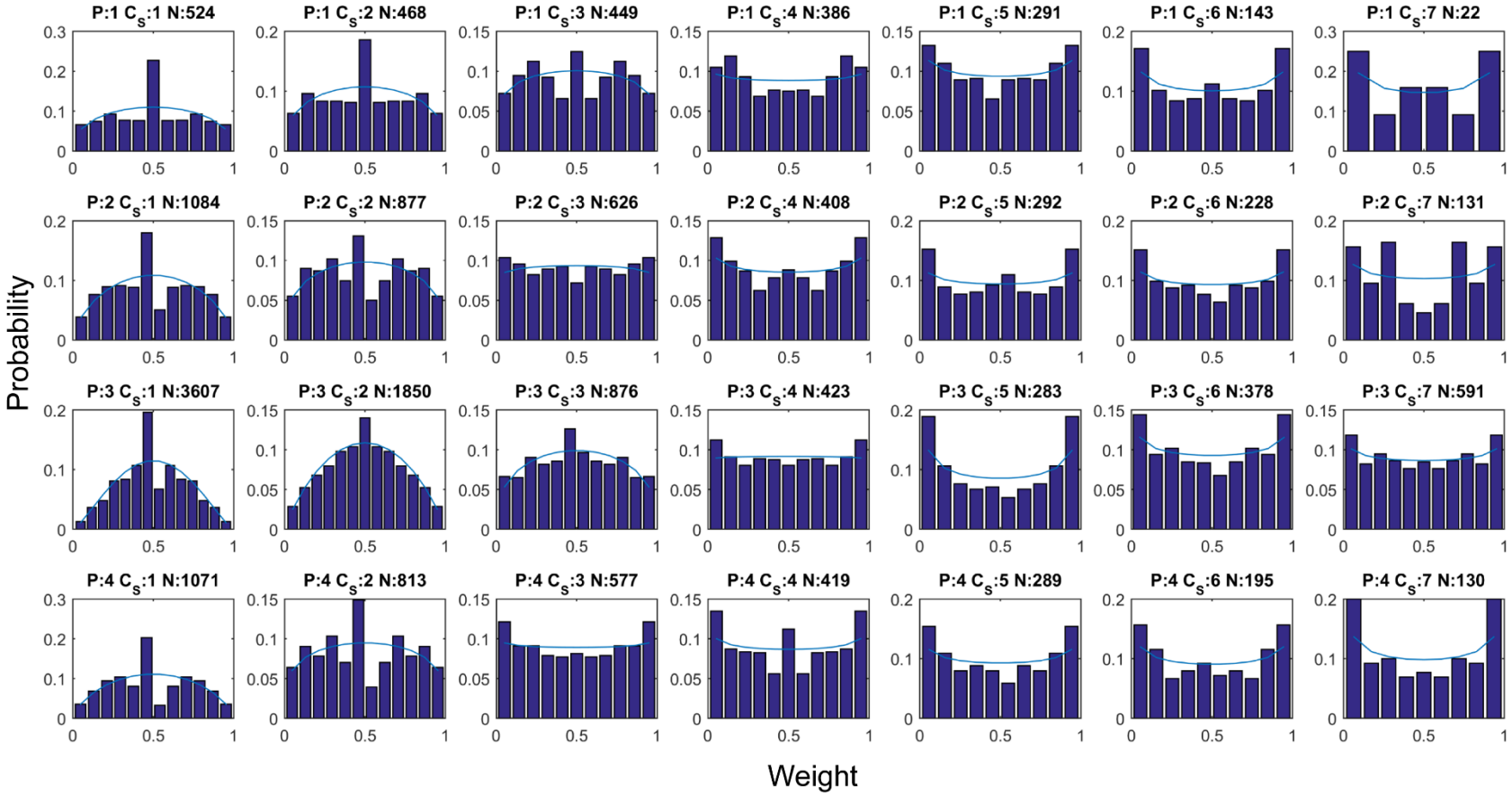

Figure S6. Same as in Figure S6 but for daily to minute- time step disaggregation.

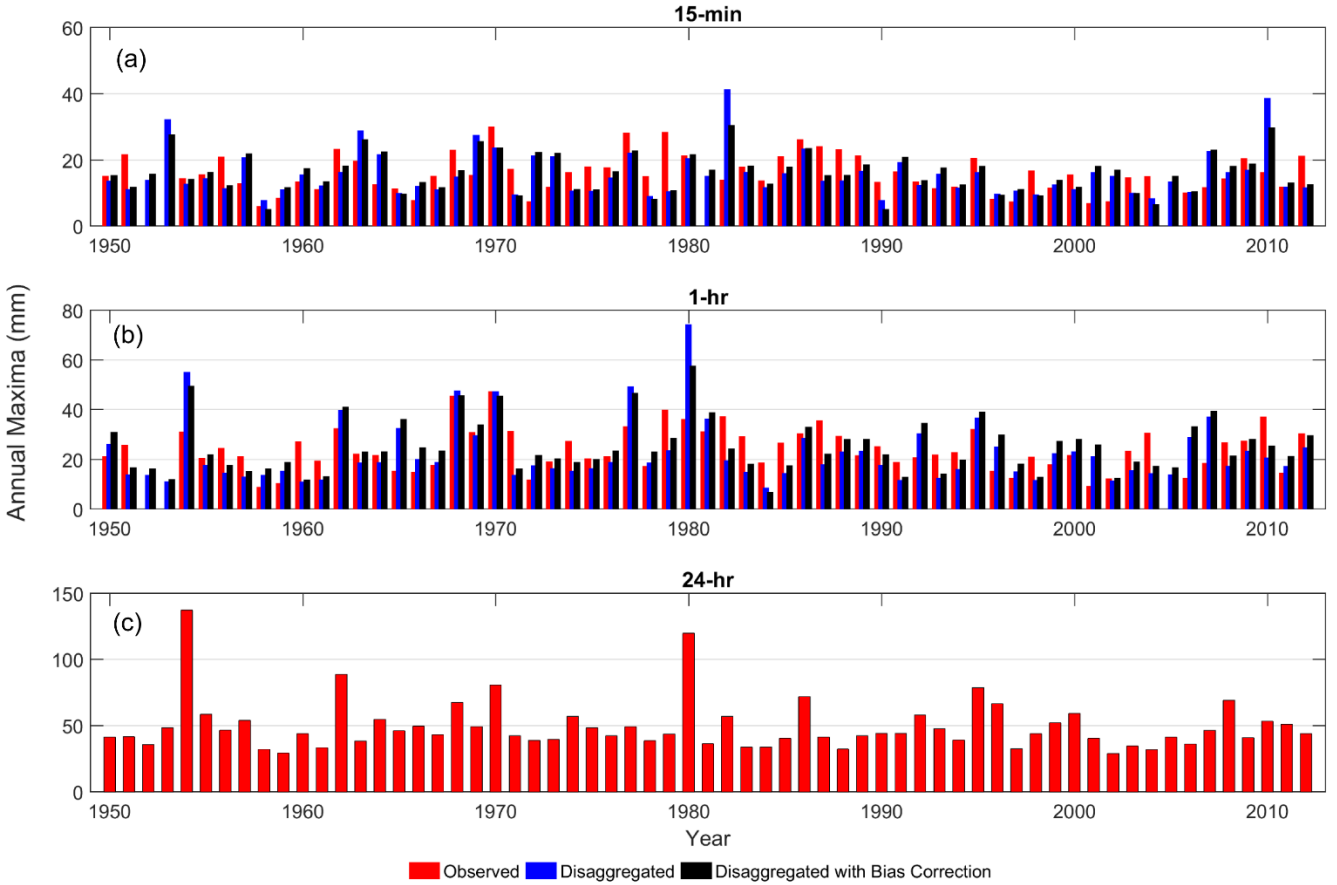

Figure S7. Comparison of observed versus disaggregated (**a**) sub-hourly and (**b)** hourly annual maximum rainfall values (Observed – red, disaggregated – blue and disaggregated and bias corrected - black) for Toronto International Airport. (**c**) The bottom panel shows AM daily rainfall values. A multiplicative random cascade-based disaggregation tool is used to disaggregate daily rainfall time series into a sub-hourly and hourly time step.

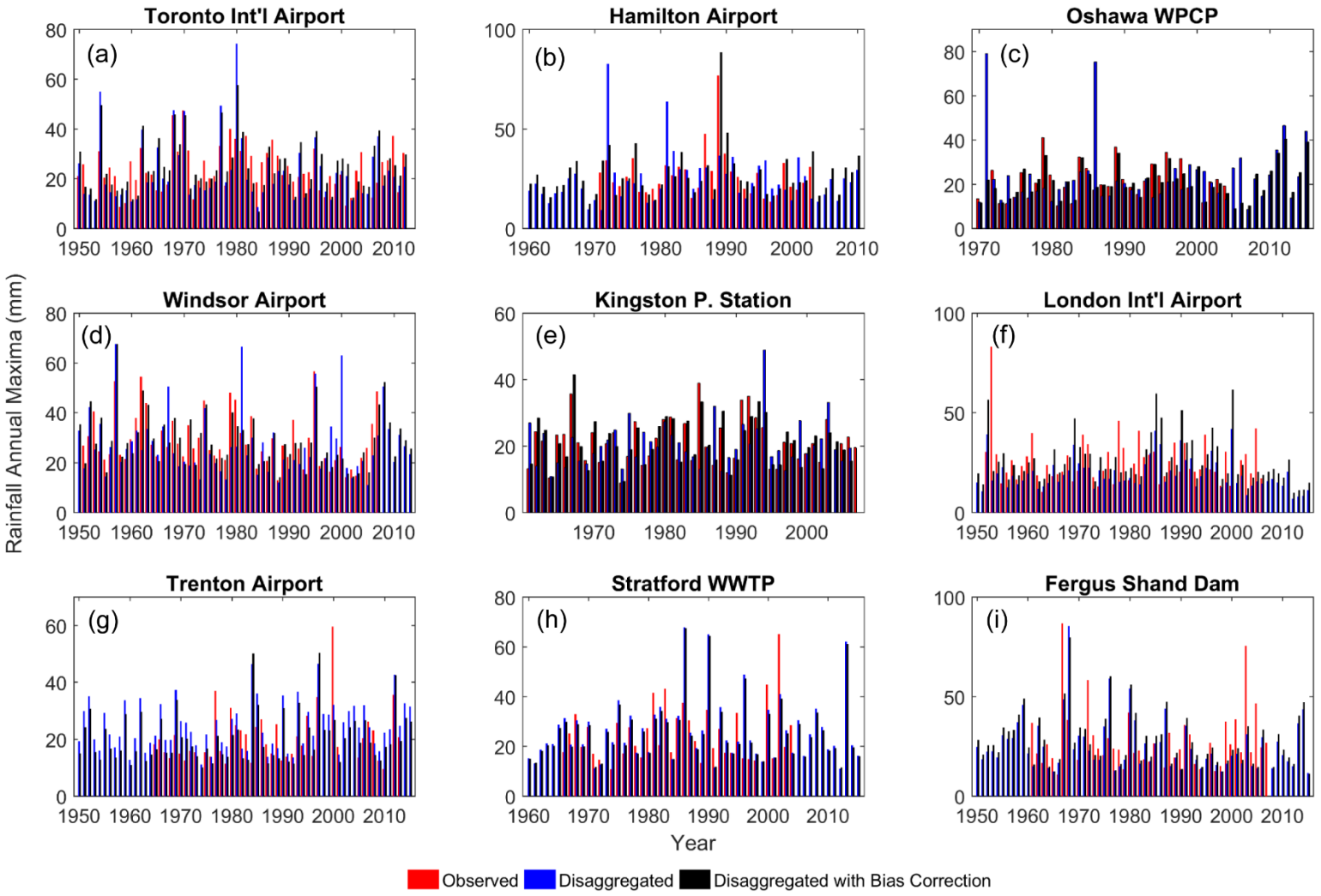

Figure S8. Comparison of observed versus disaggregated time series for 1-hour AMP in the nine locations (Observed – red, disaggregated – blue, and disaggregated and bias corrected - black): (**a**) Toronto International Airport, (**b**) Hamilton Airport, (**c**) Oshawa WPCP (**d**) Windsor Airport (**e**) Kingston P. station (**f**) London International Airport (**g**) Trenton Airport (**h**) Stratford WWTP and (**i**) Fergus Shand Dam

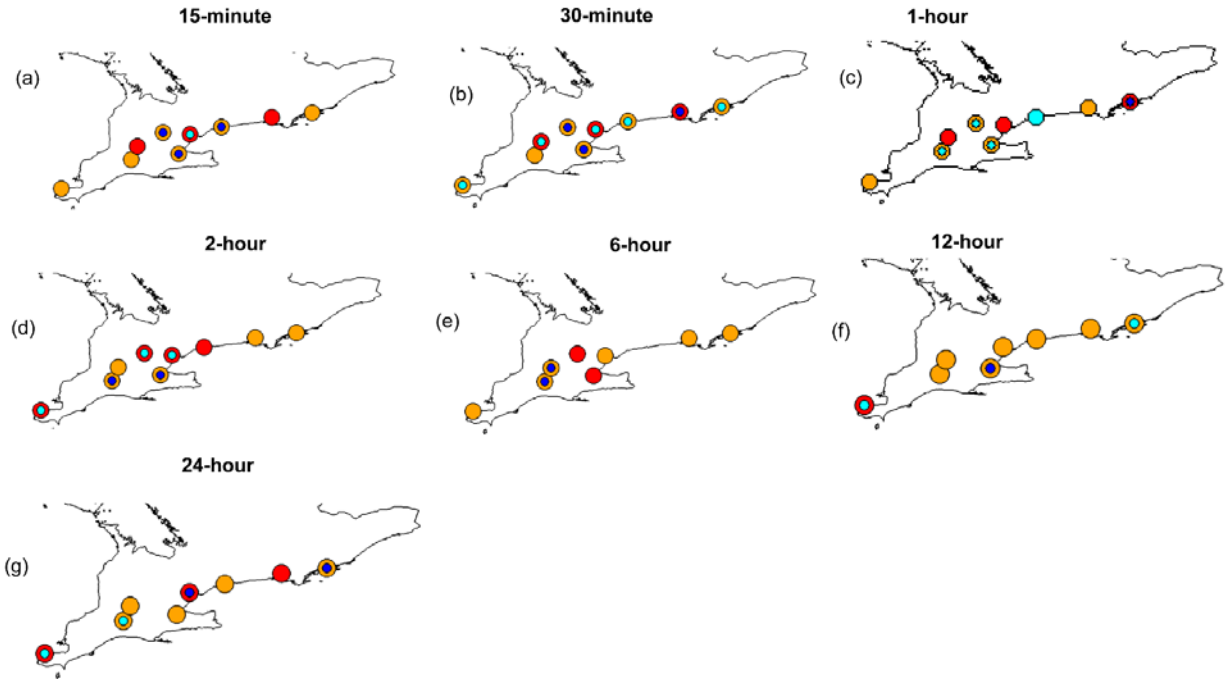

Figure S9. The performance of stationary (Blue – maximum likelihood, cyan – stationary DE-MC) versus nonstationary (Orange - nonstationary DE-MC simulation with time variant mean, red - nonstationary DE-MC simulation with time variant mean and standard deviation) GEV models with durations ranging between 15-minute and 24-hour (**a**-**g**) in nine urbanized locations. Sites with double circles indicate either better or comparable performance of the stationary versus nonstationary models and shades denote the type of the distribution.

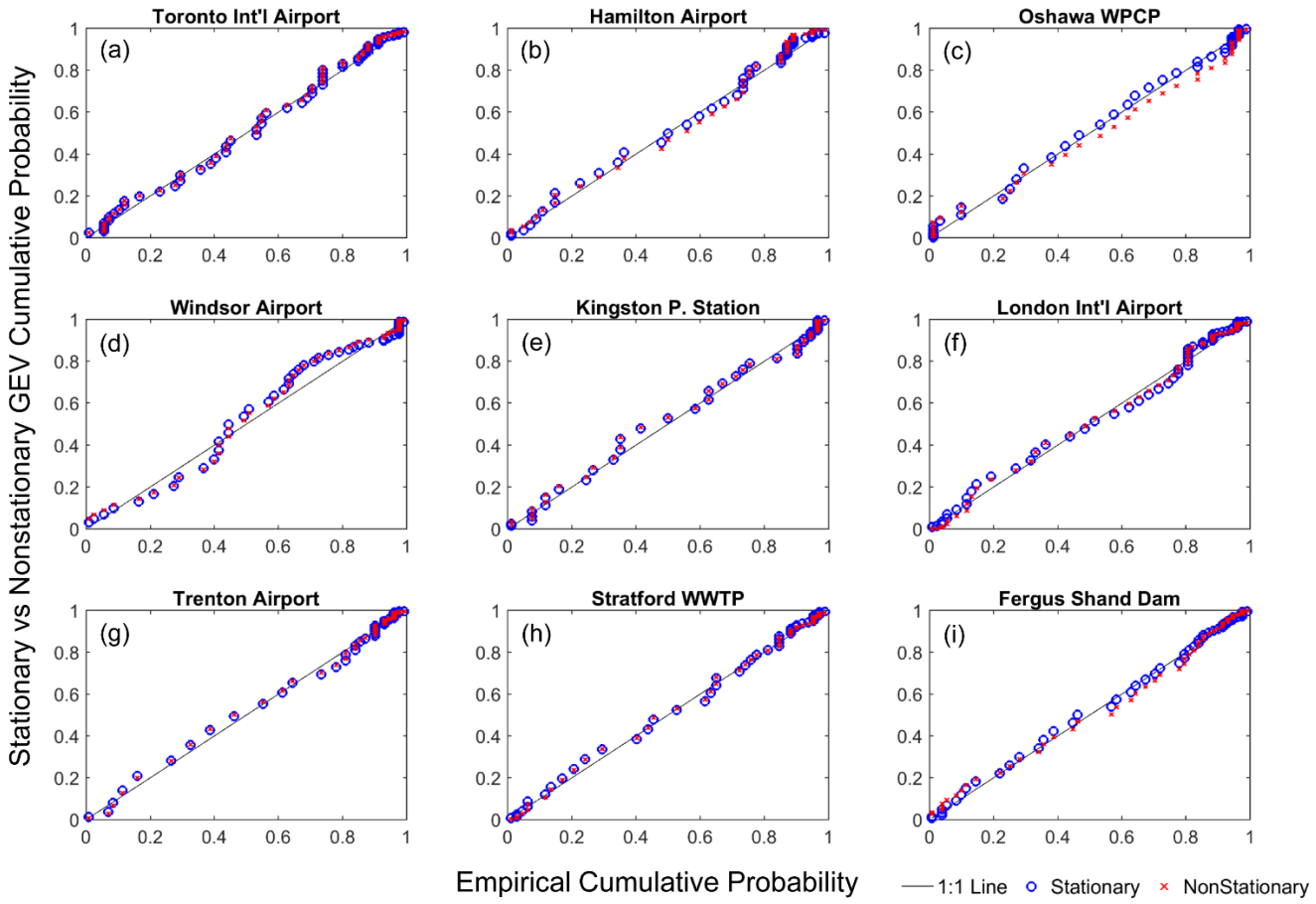

Figure S10. *PP* plots of nonstationary versus stationary GEV distributions for 15-min duration in nine sites (**a - i**): Toronto International Airport, Hamilton Airport, Oshawa WPCP, Windsor Airport, Kingston P. station, London International Airport, Trenton Airport, Stratford WWTP, and Fergus Shand Dam.

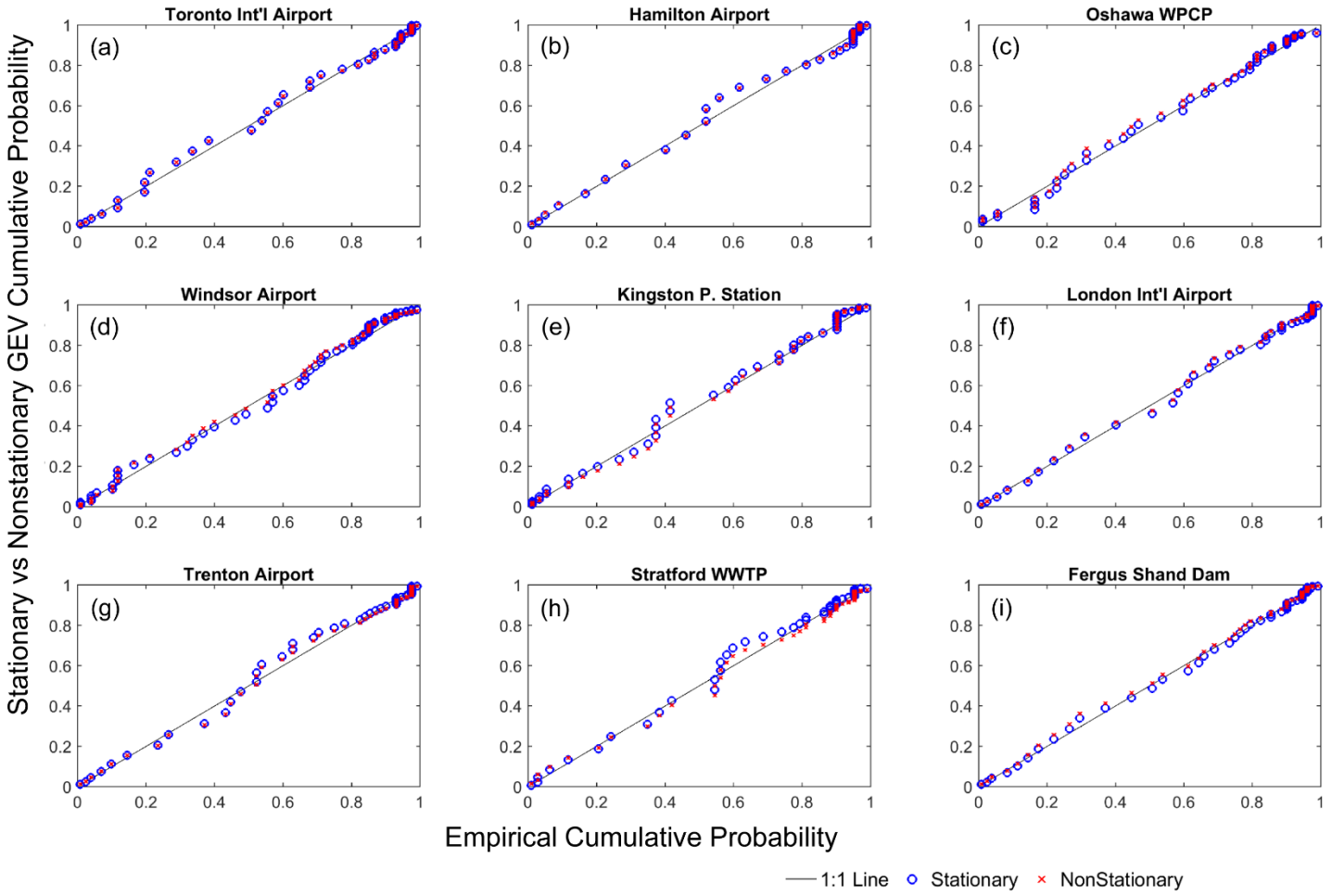

Figure S11. *PP* plots of nonstationary versus stationary GEV distributions for 1-hour duration in nine sites (**a - i**): Toronto International Airport, Hamilton Airport, Oshawa WPCP, Windsor Airport, Kingston P. station, London International Airport, Trenton Airport, Stratford WWTP, and Fergus Shand Dam.

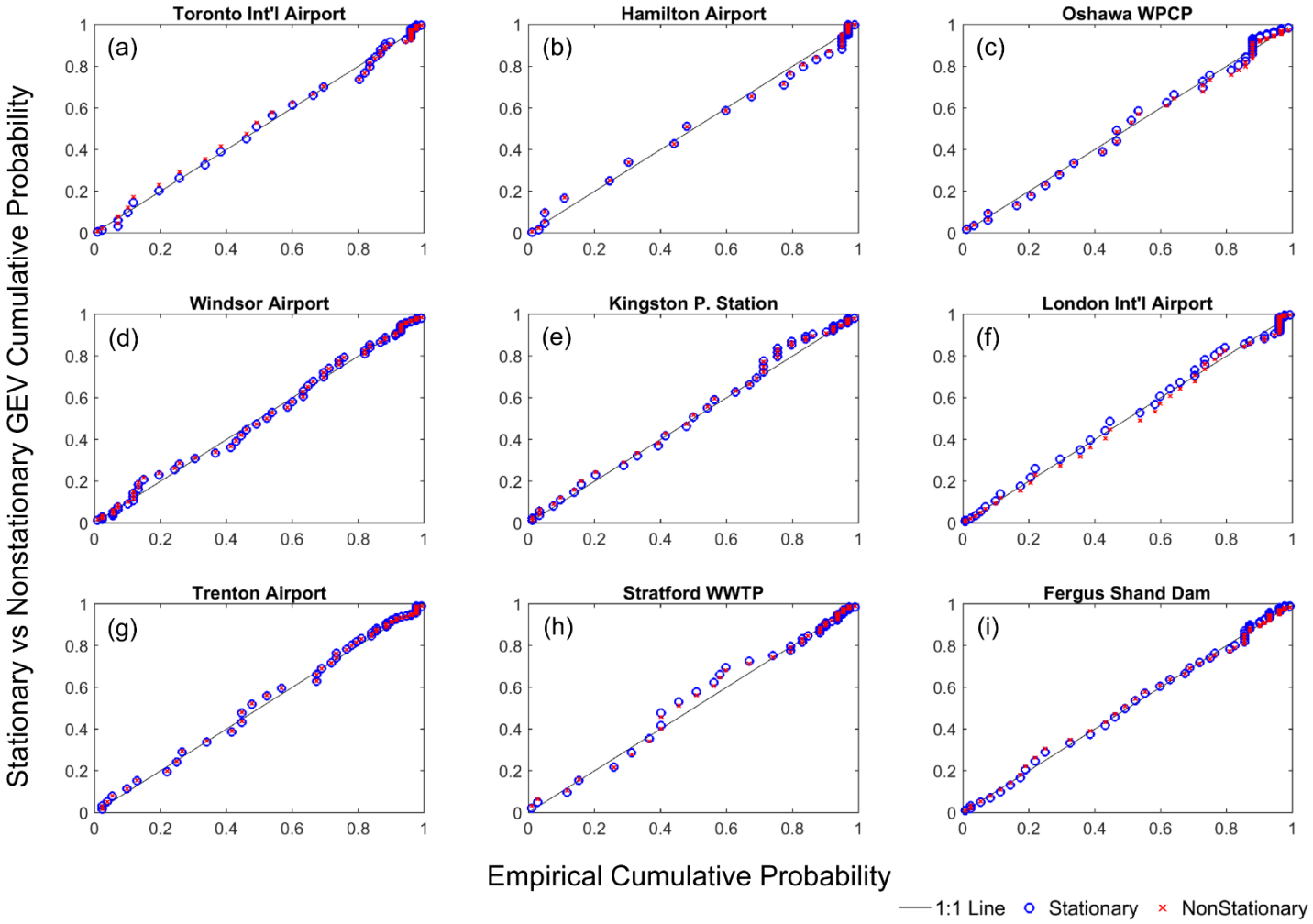

Figure S12. *PP* plots of nonstationary versus stationary GEV distributions for 2-hour duration in nine sites (**a - i**): Toronto International Airport, Hamilton Airport, Oshawa WPCP, Windsor Airport, Kingston P. station, London International Airport, Trenton Airport, Stratford WWTP, and Fergus Shand Dam.

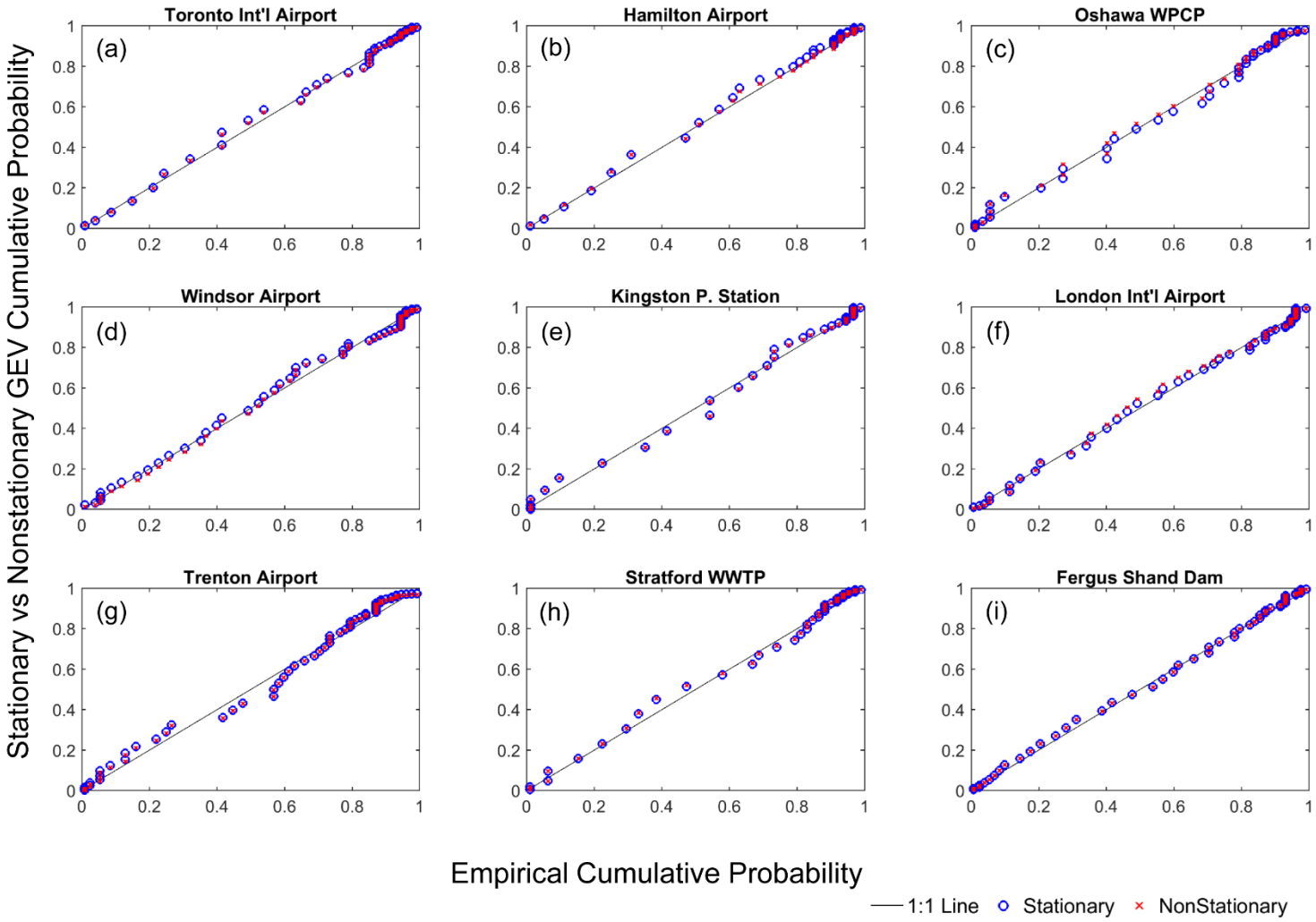

Figure S13. *PP* plots of nonstationary versus stationary GEV distributions for 6-hour duration in nine sites (**a - i**): Toronto International Airport, Hamilton Airport, Oshawa WPCP, Windsor Airport, Kingston P. station, London International Airport, Trenton Airport, Stratford WWTP, and Fergus Shand Dam.

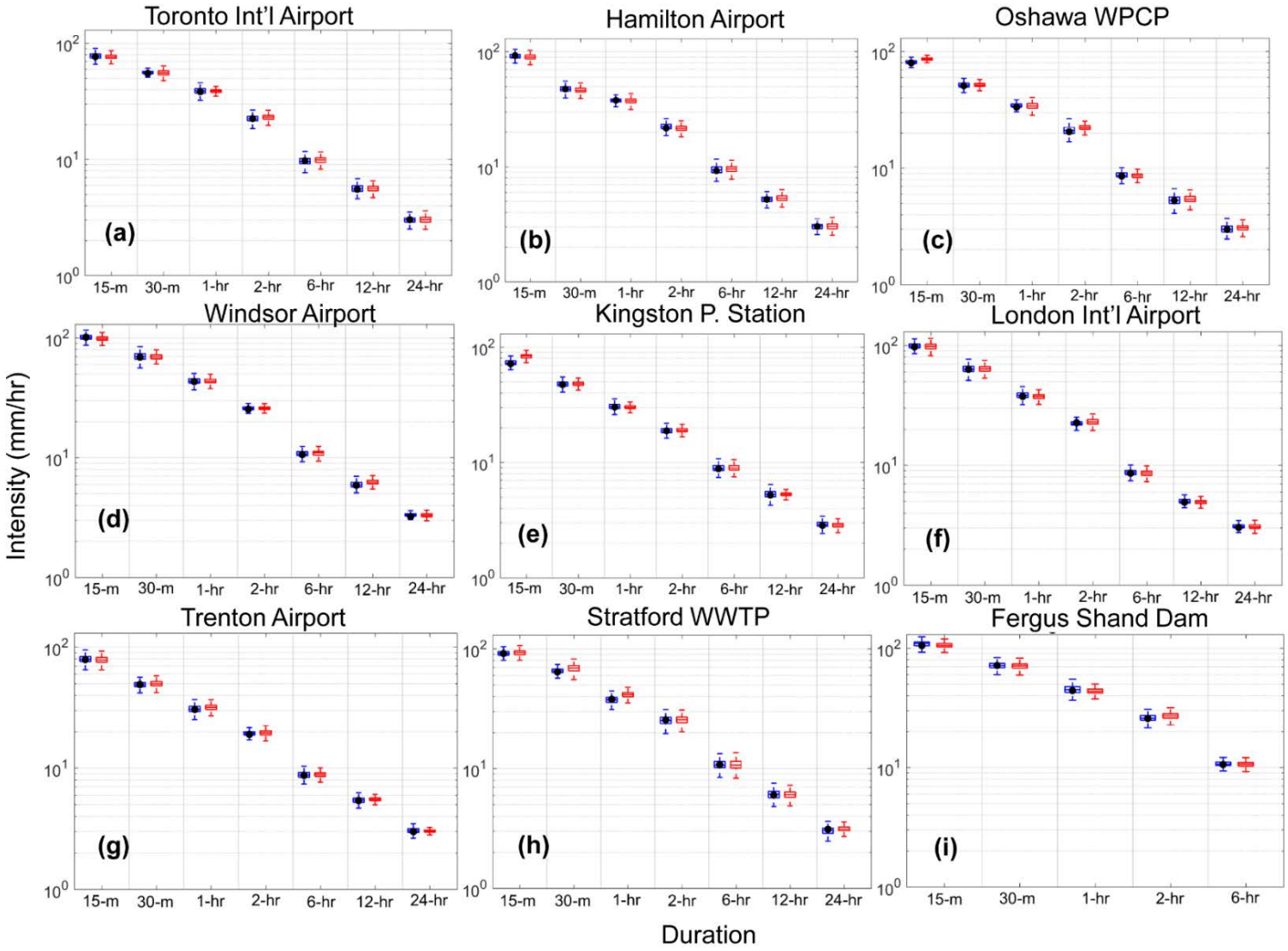

Figure S14. Uncertainty in DSI for 10-year return periods for stationary (blue) versus nonstationary (red) models with durations ranging between 15- min and 24-hr for nine sites (a - i): Toronto International Airport, Hamilton Airport, Oshawa WPCP, Windsor Airport, Kingston P. station, London International Airport, Trenton

Airport, Stratford WWTP, and Fergus Shand Dam. The boxplots indicate the uncertainty in estimated DSI from Bayesian inference, whereas the DSI obtained from maximum likelihood approach is shown as a black dot in the stationary simulation.

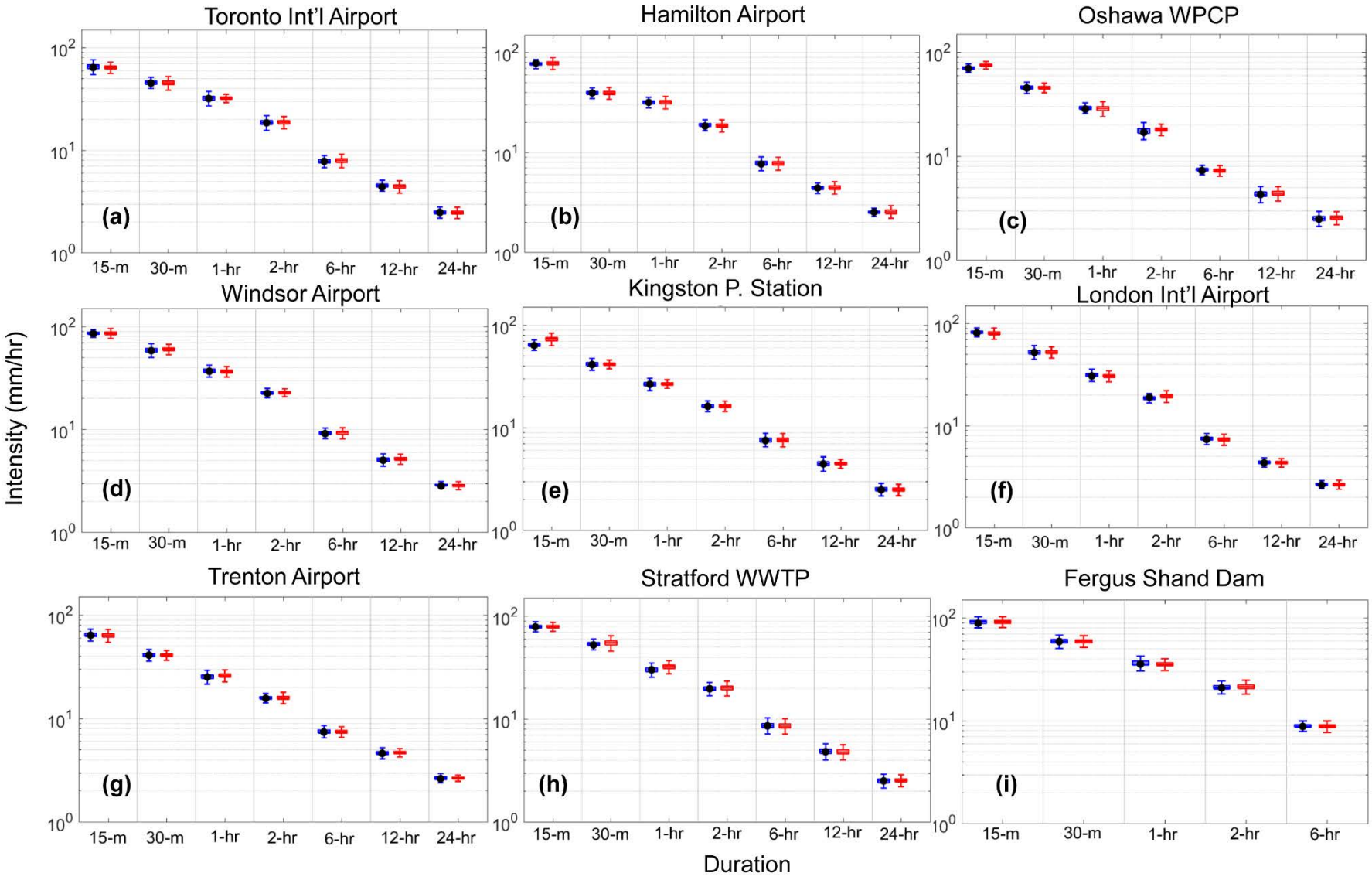

Figure S15. Same as Figure S14 but for 5-year return period.

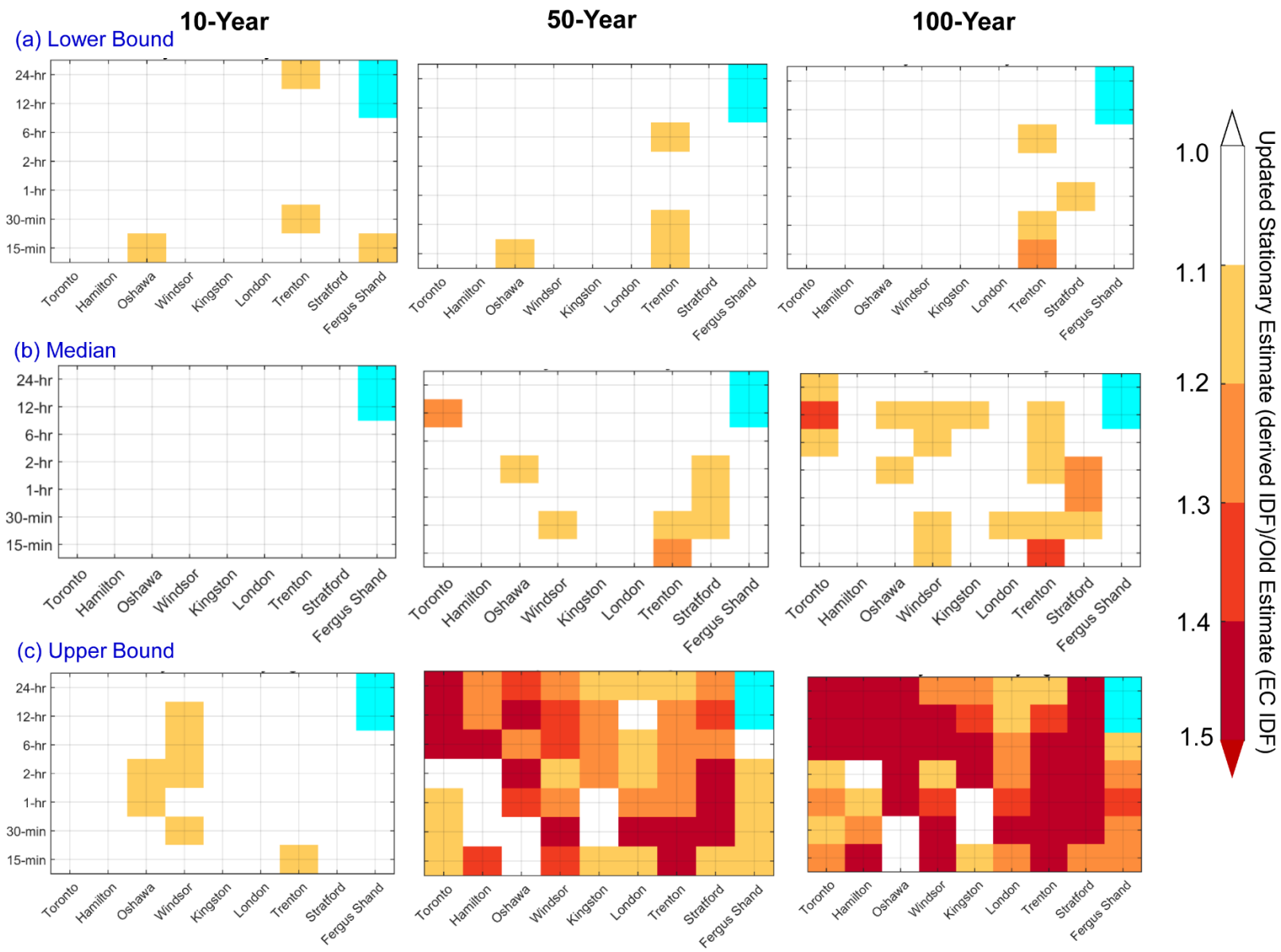

Figure S16. Same as in Figure 6 but for the updated stationary versus EC-generated *T*-year event estimates.

SI References

Akaike, H.: A new look at the statistical model identification, IEEE Trans. Autom. Control, 19(6), 716–723, 1974.

Bozdogan, H.: Akaike's information criterion and recent developments in information complexity, J. Math. Psychol., 44(1), 62–91, 2000.

ter Braak, C. J. and Vrugt, J. A.: Differential evolution Markov chain with snooker updater and fewer chains, Stat. Comput., 18(4), 435–446, 2008.

Cheng, L. and AghaKouchak, A.: Nonstationary precipitation intensity-duration-frequency curves for infrastructure design in a changing climate, Sci. Rep., 4 [online] Available from: http://www.ncbi.nlm.nih.gov/pmc/articles/PMC4235283/ (Accessed 7 September 2016), 2014.

Cheng, L., AghaKouchak, A., Gilleland, E. and Katz, R. W.: Non-stationary extreme value analysis in a changing climate, Clim. Change, 127(2), 353–369, 2014.

Coles, S., Bawa, J., Trenner, L. and Dorazio, P.: An introduction to statistical modeling of extreme values, Springer. [online] Available from: http://link.springer.com/content/pdf/10.1007/978-1-4471-3675-0.pdf (Accessed 5 January 2017), 2001.

Gelman, A., Shirley, K. and others: Inference from simulations and monitoring convergence, Handb. Markov Chain Monte Carlo, 163–174, 2011.

Gelman, A., Carlin, J. B., Stern, H. S. and Rubin, D. B.: Bayesian data analysis, Chapman & Hall/CRC Boca Raton, FL, USA. [online] Available from: http://amstat.tandfonline.com/doi/full/10.1080/01621459.2014.963405 (Accessed 6 January 2017), 2014.

Gilleland, E. and Katz, R. W.: Extremes 2.0: an extreme value analysis package in r, Submitt. J. Stat. Softw. [online] Available from: https://www.rap.ucar.edu/staff/ericg/extRemes/extRemes2.pdf (Accessed 6 January 2017), 2014.

Güntner, A., Olsson, J., Calver, A. and Gannon, B.: Cascade-based disaggregation of continuous rainfall time series: the influence of climate, Hydrol. Earth Syst. Sci. Discuss., 5(2), 145–164, 2001.

Hurvich, C. M. and Tsai, C.-L.: Model selection for extended quasi-likelihood models in small samples, Biometrics, 1077–1084, 1995.

Jebari, S., Berndtsson, R., Olsson, J. and Bahri, A.: Soil erosion estimation based on rainfall disaggregation, J. Hydrol., 436, 102–110, 2012.

Katz, R. W. and Brown, B. G.: Extreme events in a changing climate: variability is more important than averages, Clim. Change, 21(3), 289–302, 1992.

Katz, R. W., Parlange, M. B. and Naveau, P.: Statistics of extremes in hydrology, Adv. Water Resour., 25(8), 1287–1304, 2002.

Madsen, H., Arnbjerg-Nielsen, K. and Mikkelsen, P. S.: Update of regional intensity–duration–frequency curves in Denmark: tendency towards increased storm intensities, Atmospheric Res., 92(3), 343–349, 2009.

Mandelbrot, B. B.: Intermittent turbulence in self-similar cascades: divergence of high moments and dimension of the carrier, in Multifractals and 1/f Noise, pp. 317–357, Springer. [online] Available from: http://link.springer.com/chapter/10.1007/978-1-4612-2150-0_15 (Accessed 4 January 2017), 1999.

Mikkelsen, P. S., Madsen, H., Arnbjerg-Nielsen, K., Rosbjerg, D. and Harremoës, P.: Selection of regional historical rainfall time series as input to urban drainage simulations at ungauged locations, Atmospheric Res., 77(1–4), 4–17, doi:10.1016/j.atmosres.2004.10.016, 2005.

Olsson, J.: Evaluation of a scaling cascade model for temporal rain-fall disaggregation, Hydrol. Earth Syst. Sci. Discuss., 2(1), 19–30, 1998.

Olsson, J.: RANDOM CASCADE MODEL: documentation, [online] Available from: http://www.iwapublishing.com/sites/default/files/RandomCascadeModeldocumentation.docx (Accessed 4 January 2017), n.d.

Petrow, T. and Merz, B.: Trends in flood magnitude, frequency and seasonality in Germany in the period 1951–2002, J. Hydrol., 371(1), 129–141, 2009.

Rana, A., Bengtsson, L., Olsson, J. and Jothiprakash, V.: Development of IDF-curves for tropical india by random cascade modeling, Hydrol. Earth Syst. Sci. Discuss., 10(4), 4709–4738, 2013.

Renard, B., Sun, X. and Lang, M.: Bayesian methods for non-stationary extreme value analysis, in Extremes in a Changing Climate, pp. 39–95, Springer. [online] Available from: http://link.springer.com/chapter/10.1007/978-94-007-4479-0_3 (Accessed 6 January 2017), 2013.

Sen, P. K.: Estimates of the regression coefficient based on Kendall's tau, J. Am. Stat. Assoc., 63(324), 1379–1389, 1968.

Ter Braak, C. J.: A Markov Chain Monte Carlo version of the genetic algorithm Differential Evolution: easy Bayesian computing for real parameter spaces, Stat. Comput., 16(3), 239–249, 2006.

Towler, E., Rajagopalan, B., Gilleland, E., Summers, R. S., Yates, D. and Katz, R. W.: Modeling hydrologic and water quality extremes in a changing climate: A statistical approach based on extreme value theory, Water Resour. Res., 46(11), W11504, doi:10.1029/2009WR008876, 2010.

Willems, P.: Impacts of climate change on rainfall extremes and urban drainage systems, IWA Publishing. [online] Available from: https://books.google.ca/books?hl=en&lr=&id=vgCwYjhlSXkC&oi=fnd&pg=PR1&dq=Willems+et+al.+(eds),+IWA+Publishing,+2012Impacts+of+Climate+Change+on+Rainfall+Extremes+and+Urban+Drainage+Systems&ots=dQ-d_YPckD&sig=bkAqA-ixiwRTxyOuClazrb_Csys (Accessed 4 January 2017), 2012.

Yaglom, A. M.: The influence of fluctuations in energy dissipation on the shape of turbulence characteristics in the inertial interval, in Soviet Physics Doklady, vol. 11, p. 26. [online] Available from: http://adsabs.harvard.edu/abs/1966SPhD...11...26Y (Accessed 4 January 2017), 1966.

Yue, S.: A bivariate gamma distribution for use in multivariate flood frequency analysis, Hydrol. Process., 15(6), 1033–1045, 2001.

Akaike, H.: A new look at the statistical model identification, IEEE Trans. Autom. Control, 19(6), 716–723, 1974.

Bozdogan, H.: Akaike's information criterion and recent developments in information complexity, J. Math. Psychol., 44(1), 62–91, 2000.

ter Braak, C. J. and Vrugt, J. A.: Differential evolution Markov chain with snooker updater and fewer chains, Stat. Comput., 18(4), 435–446, 2008.

Cheng, L. and AghaKouchak, A.: Nonstationary precipitation intensity-duration-frequency curves for infrastructure design in a changing climate, Sci. Rep., 4 [online] Available from: http://www.ncbi.nlm.nih.gov/pmc/articles/PMC4235283/ (Accessed 7 September 2016), 2014.

Cheng, L., AghaKouchak, A., Gilleland, E. and Katz, R. W.: Non-stationary extreme value analysis in a changing climate, Clim. Change, 127(2), 353–369, 2014.

Coles, S., Bawa, J., Trenner, L. and Dorazio, P.: An introduction to statistical modeling of extreme values, Springer. [online] Available from: http://link.springer.com/content/pdf/10.1007/978-1-4471-3675-0.pdf (Accessed 5 January 2017), 2001.

Gelman, A., Shirley, K. and others: Inference from simulations and monitoring convergence, Handb. Markov Chain Monte Carlo, 163–174, 2011.

Gelman, A., Carlin, J. B., Stern, H. S. and Rubin, D. B.: Bayesian data analysis, Chapman & Hall/CRC Boca Raton, FL, USA. [online] Available from: http://amstat.tandfonline.com/doi/full/10.1080/01621459.2014.963405 (Accessed 6 January 2017), 2014.

Gilleland, E. and Katz, R. W.: Extremes 2.0: an extreme value analysis package in r, Submitt. J. Stat. Softw. [online] Available from: https://www.rap.ucar.edu/staff/ericg/extRemes/extRemes2.pdf (Accessed 6 January 2017), 2014.

Güntner, A., Olsson, J., Calver, A. and Gannon, B.: Cascade-based disaggregation of continuous rainfall time series: the influence of climate, Hydrol. Earth Syst. Sci. Discuss., 5(2), 145–164, 2001.

Hurvich, C. M. and Tsai, C.-L.: Model selection for extended quasi-likelihood models in small samples, Biometrics, 1077–1084, 1995.

Jebari, S., Berndtsson, R., Olsson, J. and Bahri, A.: Soil erosion estimation based on rainfall disaggregation, J. Hydrol., 436, 102–110, 2012.

Katz, R. W. and Brown, B. G.: Extreme events in a changing climate: variability is more important than averages, Clim. Change, 21(3), 289–302, 1992.

Katz, R. W., Parlange, M. B. and Naveau, P.: Statistics of extremes in hydrology, Adv. Water Resour., 25(8), 1287–1304, 2002.

Madsen, H., Arnbjerg-Nielsen, K. and Mikkelsen, P. S.: Update of regional intensity–duration–frequency curves in Denmark: tendency towards increased storm intensities, Atmospheric Res., 92(3), 343–349, 2009.

Mandelbrot, B. B.: Intermittent turbulence in self-similar cascades: divergence of high moments and dimension of the carrier, in Multifractals and $1/f$ Noise, pp. 317–357, Springer. [online] Available from: http://link.springer.com/chapter/10.1007/978-1-4612-2150-0_15 (Accessed 4 January 2017), 1999.

Mikkelsen, P. S., Madsen, H., Arnbjerg-Nielsen, K., Rosbjerg, D. and Harremoës, P.: Selection of regional historical rainfall time series as input to urban drainage simulations at ungauged locations, Atmospheric Res., 77(1–4), 4–17, doi:10.1016/j.atmosres.2004.10.016, 2005.

Olsson, J.: Evaluation of a scaling cascade model for temporal rain-fall disaggregation, Hydrol. Earth Syst. Sci. Discuss., 2(1), 19–30, 1998.

Olsson, J.: RANDOM CASCADE MODEL: documentation, [online] Available from: http://www.iwapublishing.com/sites/default/files/RandomCascadeModeldocumentation.docx (Accessed 4 January 2017), n.d.

Petrow, T. and Merz, B.: Trends in flood magnitude, frequency and seasonality in Germany in the period 1951–2002, J. Hydrol., 371(1), 129–141, 2009.

Rana, A., Bengtsson, L., Olsson, J. and Jothiprakash, V.: Development of IDF-curves for tropical india by random cascade modeling, Hydrol. Earth Syst. Sci. Discuss., 10(4), 4709–4738, 2013.

Renard, B., Sun, X. and Lang, M.: Bayesian methods for non-stationary extreme value analysis, in Extremes in a Changing Climate, pp. 39–95, Springer. [online] Available from: http://link.springer.com/chapter/10.1007/978-94-007-4479-0_3 (Accessed 6 January 2017), 2013.

Sen, P. K.: Estimates of the regression coefficient based on Kendall's tau, J. Am. Stat. Assoc., 63(324), 1379–1389, 1968.

Ter Braak, C. J.: A Markov Chain Monte Carlo version of the genetic algorithm Differential Evolution: easy Bayesian computing for real parameter spaces, Stat. Comput., 16(3), 239–249, 2006.

Towler, E., Rajagopalan, B., Gilleland, E., Summers, R. S., Yates, D. and Katz, R. W.: Modeling hydrologic and water quality extremes in a changing climate: A statistical approach based on extreme value theory, Water Resour. Res., 46(11), W11504, doi:10.1029/2009WR008876, 2010.

Willems, P.: Impacts of climate change on rainfall extremes and urban drainage systems, IWA Publishing. [online] Available from: https://books.google.ca/books?hl=en&lr=&id=vgCwYjhlSXkC&oi=fnd&pg=PR1&dq=Willems+et+al.+(eds),+IWA+Publishing,+2012Impacts+of+Climate+Change+on+Rainfall+Extremes+and+Urban+Drainage+Systems&ots=dQ-d_YPckD&sig=bkAqA-ixiwRTxyOuClazrb_Csys (Accessed 4 January 2017), 2012.

Yaglom, A. M.: The influence of fluctuations in energy dissipation on the shape of turbulence characteristics in the inertial interval, in Soviet Physics Doklady, vol. 11, p. 26. [online] Available from: http://adsabs.harvard.edu/abs/1966SPhD...11...26Y (Accessed 4 January 2017), 1966.

Yue, S.: A bivariate gamma distribution for use in multivariate flood frequency analysis, Hydrol. Process., 15(6), 1033–1045, 2001.